TÉCNICO LISBOA

Influence of NADH-dehydrogenases on polyhydroxyalkanoate production in *Pseudomonas taiwanensis* VLB120

João Pedro Guilherme Romba

Thesis to obtain the Master of Science Degree in

Biological Engineering

Supervisors: Prof. Leonilde de Fátima Morais Moreira and Prof. Lars M. Blank

Examination Committee

Chairperson: Prof. Duarte Miguel De França Teixeira dos Prazeres

Supervisor: Prof. Leonilde de Fátima Morais Moreira

Members of the Committee: Prof. Gabriel António Amaro Monteiro

November 2017

To my family…

Acknowledgements

First, I would like to thank Professor Birgitta Ebert for giving me the opportunity of doing my master thesis at the at the Institute of Applied Microbiology iAMB of RWTH Aachen University and PhD student Salome Nies for providing my project theme and helping and guiding with the experimental work. Without Prof. Birgitta Ebert and PhD student Salome Nies my thesis on the influence of NADH-dehydrogenases on polyhydroxyalkanoate production in *Pseudomonas taiwanensis* VLB120 would not have been possible. I'm grateful for the opportunity given and for all the hours that were invested on me. I also want to thank my Portuguese friends that were working in the institute, Ana and Dário, that helped me in this 6 months journey even if most of the times was just hearing my latest experimental mishaps in our native language, and everyone on iAMB that help me when I had a doubt or saw me puzzled by some experimental result and decided to ask me if everything was alright.

I want to thank my already graduated or soon to be Biological engineer friends that supported and helped me during my academic or personal struggles. I could always share a laugh in moments of most stress with these people.

I am grateful to my supervisor Professor Leonilde Moreira for helping in the writing process of my thesis as well as for her never ending availability and kindness.

Last but not the least, my parents and brother for always being there for me and supporting and respecting my decisions. Thank you for all the advice given and for educating me with the right set of values. I'm grateful for all the sacrifices that my family did for me and I wish I can someday repay them with interest. Finally, I would like to thank the person that is with me. In the past months, she saw all my up and downs, staying by my side when I was happy and cheerful and when I was in my worst due to stress. Besides all the advice, motivation and help, I want to thank her for never failing on putting a smile on my face independently of my mental state.

Abstract

Polyhydroxyalkanoates (PHAs) are a class of biopolymers that accumulate in the cytoplasm of bacteria when in the presence of environmental stress or when there is a high concentration of NADH inside of the cells. In this project, the influence of NADH-dehydrogenases (NHDs) on PHA production in *Pseudomonas taiwanensis* VLB120 was studied. This Pseudomonad possesses three NDHs: one NADH-dehydrogenase type I (NDH-I), encoded by the *nuo* operon, and two NADH-dehydrogenases type II (NDH-II), encoded by the *ndh* genes *PVLB_13270* and *PVLB_21880*. To study the influence of NDHs on PHA production, several *P. taiwanensis* VLB120 NDHs mutants were used. First, the working strains were submitted to a growth characterization to determine if the NDHs mutations affected the cells. Only *P. taiwanensis* VLB120*ΔΔndh* had its metabolism altered. Since mutants were cultivated in minimal medium without stress, there was the possibility that cells could consume the PHAs if produced. Therefore, strains were submitted to the knockout of the PHA depolymerase gene (*phaZ*) to guarantee no PHA degradation. Obtained results confirmed the presence of PHA granules inside the NDH mutant strains by using fluorescence microscopy. Finally, a relative quantification of PHAs was conducted using two different methods, a Nile Red stain rapid method and gas chromatography-mass spectrometry (GC-MS). The Nile Red rapid method proved to be inadequate. The experiment using GC-MS has shown that all NDHs mutant strains VLB120*Δ13270ΔphaZ*, VLB120*Δ21880ΔphaZ*, VLB120*ΔnuoΔphaZ*, VLB120*ΔΔndhΔphaZ* and VLB120*ΔnuoΔ13270ΔphaZ* produced, respectively, 60%, 109%, 181%, 264% and 379% more than the wildtype, confirming the role of NDHs in increasing PHAs biosynthesis.

Keywords: *P. taiwanensis* VLB120, NADH-dehydrogenases, Polyhydroxyalkanoates, Nile Red, GC-MS

Resumo

Polihidroxialcanoatos (PHAs) são biopolímeros que se acumulam no citoplasma de bactérias quando há stresse ambiental, ou uma elevada concentração de NADH, e excesso de carbono. O objetivo deste projeto consistiu em estudar a influência de NADH-desidrogenases (NDHs) na produção de PHAs em *Pseudomonas taiwanensis* VLB120. A estirpe usada possui três NDHs: uma NADH-desidrogenase tipo I (NDH-I), codificada pelo operão *nuo*, e duas NADH-desidrogenases tipo II (NDH-II), codificadas pelos genes *PVLB_13270* e *PVLB_21880*. Para estudar a influência das NDHs na produção de PHAs foram testadas estirpes de *P. taiwanensis* VLB120 com mutações nessas NDHs. Inicialmente, caracterizou-se o crescimento das estirpes para verificar se as mutações nas NDHs afetavam as células. Apenas *P. taiwanensis* VLB120*ΔΔndh* teve o metabolismo afetado. Dado os mutantes terem sido cultivados na ausência de stress, as células poderiam consumir os PHAs caso esses fossem produzidos. Assim, eliminou-se o gene que codifica a PHA depolimerase (*phaZ*) em todos os mutantes para garantir a não degradação de PHAs. Resultados obtidos por microscopia de fluorescência, confirmaram a presença de grânulos de PHAs nos mutantes. A quantificação relativa da produção de PHAs foi efectuada por dois métodos - um método rápido envolvendo Vermelho de Nilo e outro que consiste em cromatografia gasosa associada a espectrometria de massa (GC-MS). O método rápido provou ser inadequado. A quantificação por GC-MS mostrou que os mutantes VLB120*Δ13270ΔphaZ*, VLB120*Δ21880ΔphaZ*, VLB120*ΔnuoΔphaZ*, VLB120*ΔΔndhΔphaZ* e VLB120*ΔnuoΔ13270ΔphaZ* produziram respetivamente, 60%, 109%, 181%, 264% e 379% mais que a estirpe selvagem, confirmando o envolvimento das NDHs no aumento da biossíntese de PHAs.

Palavras-chave: *P. taiwanensis* VLB120, NADH-desidrogenases, Polihydroxialcanoatos, Vermelho de Nilo, GC-MS

List of Contents

List of Figures

List of Tables

Nomenclature

A_{IS}	Area of the chromatogram corresponding to the IS peak
A_{PHA}	Area of the chromatogram corresponding to the PHA peak (C_8 or C_{10})
bp	Base pairs
C_8	3-hydroxyoctanoate
C_{10}	3-hydroxydecanoate
DMSO	Dimethyl sulfoxide
DNA	Deoxyribonucleic acid
ECT	Electron chain transport
EI	Electron ionization
FeS	Iron sulfer clusters
FAD	Flavin adenine dinucleotide
FMN	Flavin mononucleotide
fwd	Forward
GC-MS	Gas chromatography-mass spectrometry
H_n^+	Protons taken from the negative inner side of the membrane
H_p^+	Protons in the positive side of the membrane
IS	Internal standard
kDa	Kilo Dalton
K_m	Michaelis constant
lcl	Long chain length
mcl	Medium chain length
MCS	Multiple cloning site
MSTFA	N-methyl-N-(trimethylsilyl) trifluoroacetamide
NAD^+/NADH	Nicotinamide adenine dinucleotide
$NADP^+$/NAPH	Nicotinamide adenine dinucleotide phosphate
NDH	NADH-dehydrogenase
NDH-I	NADH-dehydrogenase type I
NDH-II	NADH-dehydrogenase type II
NQR	Sodium-pumping NADH-dehydrogenase
OD_{600}	Optical density measured at a wavelength of 600 nm
PCR	Polymerase chain reaction
PEG	Polyethylen glycol
PHA	Polyhydroxyalkanoate
PHB	Poly-3-hydroxybutyrate
Q	Ubiquinone
rev	Reverse
rpm	Rotations per minute
scl	Small chain length
TCA cycle	Tricarboxylic acid cycle
t_e	Elongation time
T_m	Annealing temperature
TS1	Downstream region of the target gene
TS2	Upstream region of the target gene

1. Introduction

Polyhydroxyalkanoates (PHAs) are a group of natural polymers produced by several microorganisms. Nonetheless, the synthesis of the polymer generally only occurs when the cells are under environmental stresses as well as an excess of carbon (Ren *et al.*, 2009). The metabolic pathways of PHAs are interconnected into several pathways belonging to the central metabolic metabolism, and it is believed that the concentration of the cofactor NADH inside the cells also influences the production of PHAs. NADH-dehydrogenases catalyze the oxidation of NADH to NAD^+ and, depending on the species of bacteria, the number of NADH-dehydrogenases and their type can vary. It is suspected that deleting particular NADH-dehydrogenases from the genome of certain bacteria species will cause an increase of the NADH concentration and ultimately stimulate the production of PHAs without the presence of environmental stress (Escapa *et al.*, 2012).

In this project, the influence of NADH-dehydrogenases in PHA production on *Pseudomonas taiwanensis* VLB120 was studied. In the following sections of this thesis, it is possible to find a detailed introduction of the key aspects for the understanding of the present investigation.

1.1. *Pseudomonas taiwanensis* VLB120

Pseudomonas taiwanensis VLB120 is a strictly aerobic, Gram-negative, rod-shaped, and motile bacterium that has been assigned to the genus *Pseudomonas* of the class Gammaproteobacteria, family Pseudomonadaceae. The microorganism was first isolated on the University of Stuttgart, in 1998, from forest soil by using styrene as sole carbon and energy source (Köhler *et al.*, 2013).

P. taiwanensis VLB120 can use a wide variety of carbon sources, including short and mid-chain length alcohols and it is capable of growing in the presence of a second phase of toxic organic solvents, such as octanol, toluene and styrene. The complete genome of this microorganism was sequenced and, within the genetic information gathered, two solvent resistant pumps were found, homologous to two well-characterized organic solvent efflux pumps (TtgABC and TtgGHI) from *Pseudomonas putida* DOT-T1E. Additionally, genetic data regarding other solvent tolerance mechanisms, such as alterations in the glycerophospholipid composition of the membrane, was discovered. This points for a wider variety of toxic solvents that cells of this strain can tolerate (Köhler *et al.*, 2013). Additionally, *P. taiwanensis* VLB120 is capable of forming biofilms, making the bacterial cells more resistant to environmental stresses, such as antimicrobial substances, heavy metals, toxic chemicals and organic acids, when compared to planktonic or freely swimming cells. These resistances make biofilms promising catalysts in long-term conversions since this system benefits from natural self-immobilisation and regeneration, long-term stability, continuous fine chemical production and it also increases the resistance of the cells to toxic compounds (Halan *et al.*, 2011).

These traits make *P. taiwanensis* VLB120 a potential candidate for applications on industrial biotransformation processes. For example, this Pseudomonad is used to efficiently catalyse the

epoxidation of the toxic substrate styrene into *(S)*-styrene, which is an important intermediate in the synthesis of fine chemicals and pharmaceuticals (Choudhary *et al*., 2006; Kreuter, 1996; Volmer *et al.*, 2014). However, since *P. taiwanensis* VLB120 can assimilate styrene as a carbon and energy source, the mutant strain *P. taiwanensis* VLB120*ΔC* was created by deleting the *styC* gene that codes the styrene oxide isomerase. In the literature, the efficient biotransformation from styrene into *(S)*-styrene using this mutant strain is described in bioprocesses using stirred tank reactors and biofilm reactors (Halan *et al.*, 2011). Another application of the strain *P. taiwanensis* VLB120 is the possibility of using lignocellulosic substrates as an alternative feedstock since it can naturally degrade xylose. This alternative lignocellulosic substrate is a mixture of hexoses (e.g., D-glucose), organic acids (e.g. acetate and formate) and pentose sugars (e.g. D-xylose and L-arabinose). In contrary to other *Pseudomonas* strains with industrial potentials, such as *P. putida* KT2440, *P. putida* DOT-T1E and *P. putida* S12, *P. taiwanensis* VLB120 is the only one described solvent-tolerant Pseudomonads with the ability to grow on xylose as sole carbon and energy source (Köhler *et al.*, 2015).

P. taiwanensis VLB120 is a solvent-tolerant, biofilm-forming strain that has a high potential for industrial applications. However, the most important characteristic for the present investigation is the quantity and type of NADH-dehydrogenases that this Pseudomonad possesses. This strain has a total of three NADH-dehydrogenases of two different types. One NADH-dehydrogenase of type I, encoded by the *nuo* operon (*PVLB_15600-15660*), and two NADH-dehydrogenases of type II, encoded by the genes *PVLB_13270* and *PVLB_21880*.

1.2. NADH-dehydrogenases in bacteria

The vast majority of bacteria have a respiratory chain, also known as electron transport chain (ECT), constituted by dehydrogenases and cytochromes. This system is located in the cytoplasmic membrane of the cells and has the primary purpose of generating energy. The transport of electrons is carried out between the constituents of the respiratory chain in a succession of redox reactions. At the same time, there is the passage of electrons as well as the translocation of protons across the plasma membrane by some of the constituents in the respiratory chain. The electrochemical gradient created generates a proton motive force that activates the ATP synthase producing ATP (Friedrich *et al.*, 2000).

The dehydrogenases have flavoprotein enzymes that transfer the electrons to the cytochrome system. The cytochromes in aerobic bacteria are characterised by a significant diversity, as shown in figure 1 (Gel'man *et al.*,1967).

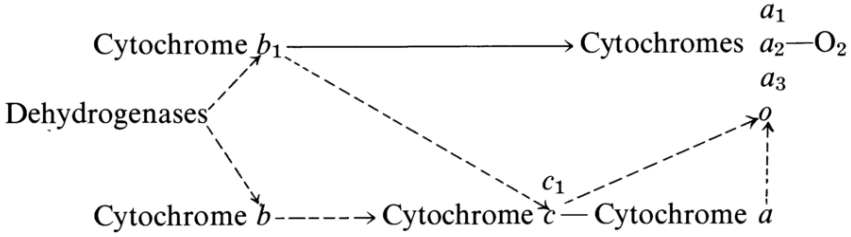

Figure 1. Possible pathways of electron transport in bacterial cytochrome systems (Gel'man *et al.*,1967).

Cytochromes with different prosthetics groups, such as *a*, *b*, *c* or *o*, are present in bacterial respiratory chains. Ubiquinones help the transportation of electrons between the components. However, the pathway that the electrons describe between cytochromes varies depending on bacterial species. For example, in *Pseudomonas aeruginosa* growing in aerobic conditions, the electron path is suggested to be in the following order: primary dehydrogenase, *c*, *c1*, *c*, *o* and oxygen (Matsushita *et al.*, 1980).

The first components in the respiratory chain usually are NADH-dehydrogenases. These enzyme complexes serve as the primary entry point of electrons by oxidising NADH. Most bacteria use a variety of NADH-dehydrogenases to deliver electrons from the central metabolism into the respiratory chain. There are three types of NADH-dehydrogenases found in microorganisms that vary in terms of evolutionary origin, catalytic mechanism, subunit composition and protein structure (Heikal *et al.*, 2014). The different dehydrogenases are the proton-pumping type I NADH dehydrogenase (NDH-I, complex I), the non-proton pumping type II NADH-dehydrogenase (NDH-II) and the pumping sodium-pumping NADH-dehydrogenase (NQR) (Kerscher *et al.*, 2008).

Some organisms might have encoded in their genome different combinations of these three types of NADH-dehydrogenases and can have more than one NDH-II type enzyme (Kerscher *et al.*, 2008). Since the microorganism studied in this research work, *P. taiwanensis* VLB120, has only two types of NADH-dehydrogenases, NDH-I and NDH-II, only these two types of enzymes are going to be described in more detail in the following sections.

1.2.1. NADH-dehydrogenase type I

The proton-pumping NADH-dehydrogenase type I, otherwise known as NADH: ubiquinone oxidoreductase or respiratory complex I is the most complex of the three NADH-dehydrogenases. Complex I is characterised by its prosthetic groups, namely a flavin mononucleotide (FMN) and up to nine iron-sulphur (FeS) clusters, its large number of subunits, as well as its sensitivity to a variety of natural compounds like rotenone or piericidin A (Friedrich *et al.*, 2000).

The multisubunit complex I catalyses the transfer of electrons from NADH to a ubiquinone and, at the same time, promotes translocation of protons across the membrane, as it can be seen in figure 2 and according to the following reaction:

$$\mathrm{NADH} + \mathrm{Q} + 5\mathrm{H}_\mathrm{n}^+ \rightarrow \mathrm{NAD}^+ + \mathrm{QH}_2 + 4\mathrm{H}_\mathrm{p}^+, \textbf{(1)}$$

where Q is the ubiquinone, and H_n^+ and H_p^+ the protons taken from the negative inner side and delivered to the positive outer side of the cell membrane.

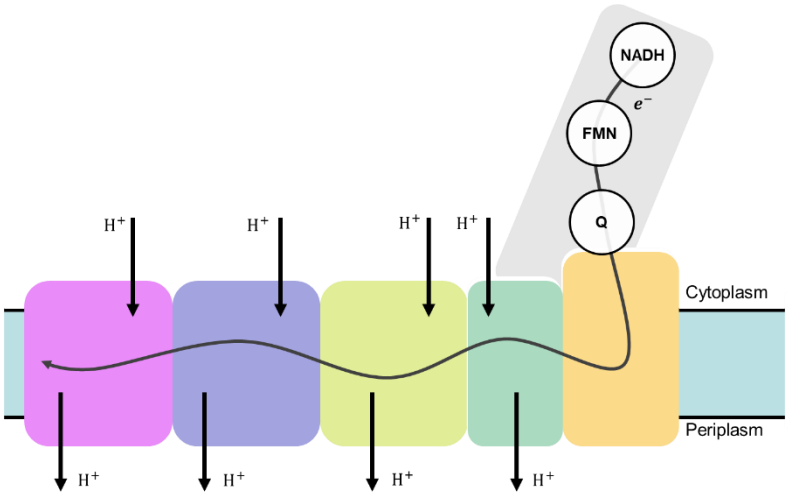

Figure 2. Structure of the bacterial NADH-dehydrogenase type I. Several subunits are not represented. Adapted from the work of Berrisford and collaborators (Berrisford *et al.*, 2016).

Homologue enzymes of complex I exist in bacteria, archaea and eukarya (Friedrich *et al.*, 2000). This complex in bacteria, such as *Escherichia coli* and *Salmonella typhimurium*, consist of 14 subunits with a total mass of 550 kDa. The 14 genes that encode the subunits are located in the *nuo* operon (Kerscher *et al.*, 2008). In eukaryotic cells the enzyme is far more complicated than in bacteria cells, reaching in bovine cells up to 45 different subunits and at least 40 different units in fungi such as the yeast *Yarrowia lipolytica*. All 14 subunits of the complex I in bacteria are integrated into the more complex eukaryotic dehydrogenase (Archer *et al.*, 1995).

1.2.2. NADH-dehydrogenase type II

In comparison to the other two families of NADH-dehydrogenases, NDH-II type enzymes do not contribute to the formation of the proton electrochemical gradient across the membrane. These dehydrogenases are usually a single polypeptide chain, coded by the *ndh* gene, with a molecular mass between 50 and 60 kDa (figure 3). It catalyses the electron transfer from a NADH molecule via a flavin adenine dinucleotide (FAD), as a redox prosthetic group, to a quinone:

$$\mathrm{NADH} + \mathrm{Q} \rightarrow \mathrm{NAD^+} + \mathrm{QH_2}, \textbf{ (2)}$$

where Q is the quinone (Kerscher *et al.,* 2008).

NDH-II is present in bacteria, and it is found in mitochondria of fungi, plants and some protists. However, this dehydrogenase has not been reported in mammalian mitochondria and is mainly found in bacterial pathogens, which suggests that these enzymes may represent a potential drug target for the treatment of human pathogens (Heikal *et al.*, 2014).

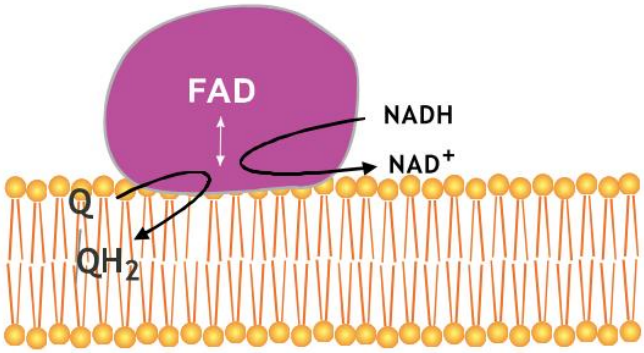

Figure 3. Structure of the bacterial NADH-dehydrogenase of type II (Kerscher *et al.*, 2008).

1.3. Polyhydroxyalkanoates (PHAs)

PHAs are bioplastic substances that were first discovered by Lemoigne in 1926 and since then they attracted much commercial and research interests due to its biodegradability, biocompatibility, chemical-diversity, and it's manufacturing procedures that make use of renewable carbon sources. These environmental friendly polymers can be used as an alternative material to conventional petrochemical-based plastics (Tan *et al.*, 2014).

From a biological point of view, PHAs serve a vital role in the survival capacities of microorganisms. These polymers are accumulated in the cytoplasm as reserve storage granules and promote the bacteria's long-term survival by serving as a carbon and reducing power reserve (figure 4). They are generally produced under unfavourable growth conditions, more specifically when there is an excess of carbon source and the absence of essential growth nutrients, typically nitrogen, phosphate, sulphur or oxygen. The polyesters are then degraded when the environmental stress is released. Accumulation of PHAs are also believed to occur when there is a high ratio of [NADH/NAD] and [acetyl-CoA /CoA] (Ren *et al.*, 2009).

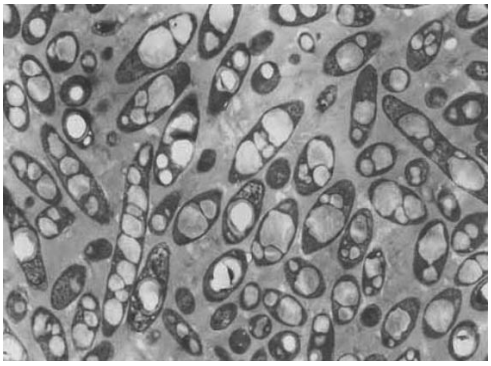

Figure 4. Transmission electron micrograph of recombinant *Escherichia coli* XL1-Blue cells with the plasmid pSYL105. PHA granules are clearly seen inside the cells (Lee *et al.*, 1996).

The general structure of PHA monomer is shown in figure 5. Each monomer has a side chain *R* that can take several forms, such as an unsaturated alkyl group. The different structures that the monomer can take, more specifically the side chain, is dependent on the microorganism and on the

substrate that the cells are using to grow. So far, over 150 monomers of various structures have been reported (Cheng *et al.*, 2016). The number of repeating units on each polymer chain, on average, goes between 100 to 30,000 units (Jiang *et al.*, 2016), resulting in polymer molar masses ranging from 50,000 to 1,000,000 Da (Reddy *et al.*, 2003). The PHA classification is determined by the total number of carbon atoms within a PHA monomer (figure 5). The biopolymer can be designed as either short-chain length PHA (scl-PHA; 3 to 5 carbon atoms), medium-chain length PHA (mcl-PHA; 6 to 12 carbon atoms), or long-chain length PHA (lcl-PHA, 13 or more carbon atoms) (Ren *et al.,* 2009).

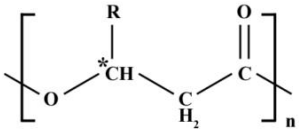

Poly(3-hydroxyalkanoate)

R group	Carbon no.	PHA polymer
methyl	C_4	Poly(3-hydroxybutyrate)
ethyl	C_5	Poly(3-hydroxyvalerate)
propyl	C_6	Poly(3-hydroxyhexanoate)
butyl	C_7	Poly(3-hydroxyheptanoate)
pentyl	C_8	Poly(3-hydroxyoctanoate)
hexyl	C_9	Poly(3-hydroxynonanoate)
heptyl	C_{10}	Poly(3-hydroxydecanoate)
octyl	C_{11}	Poly(3-hydroxyundecanoate)
nonyl	C_{12}	Poly(3-hydroxydodecanoate)
decyl	C_{13}	Poly(3-hydroxytridecanoate)
undecyl	C_{14}	Poly(3-hydroxytetradecanoate)
dodecyl	C_{15}	Poly(3-hydroxypentadecanoate)
tridecyl	C_{16}	Poly(3-hydroxyhexadecanoate)

Figure 5. PHA chemical structure. The nomenclature and carbon number for PHA compounds is determined by the functional alkyl *R* group. Asterisk denotes the chiral center of PHA-building block (Tan *et al.,* 2014).

As an example of what was mention before regarding the monomer structure, *Pseudomonas* strains only produce mcl-PHAs and, depending on the carbon source, the type of PHA monomers produced can vary. In the work of Huijeverts and collaborators, *P. putida* KT2442 cells were grown in several carbon sources. When the bacteria were grown in glucose, the primary monomers synthesised were 3-hydroxydecanoates, but when the cells were fed with decanoate as a carbon source, the majority of monomers were 3-hydroxyoctanoate (Huijberts *et al.*, 1992).

1.4. Polyhydroxyalkanoates metabolic pathways

The current knowledge on the biosynthetic pathways of PHAs is mainly concentrated on the synthesis of scl-PHAs and mcl-PHAs monomers. The research on lcl-PHAs falls short when comparing to other types of PHA monomers, remaining still much about the biosynthetic pathways to be uncovered (Tan *et al.*, 2014). Thus, this chapter will be mainly focused on the metabolic pathways of scl-PHAs and mcl-PHAs. All the information mentioned in this section will be only referred to these two types of polymers.

PHA biosynthetic pathways are intricately connected with bacterium's central metabolic pathways including glycolysis, TCA cycle, β-oxidation, *de novo* fatty acid synthesis, amino acid catabolism and Calvin Cycle (figure 6). Several common intermediates are shared between the PHA metabolism and these metabolic pathways, specially acetyl-CoA (Escapa *et al.*, 2012).

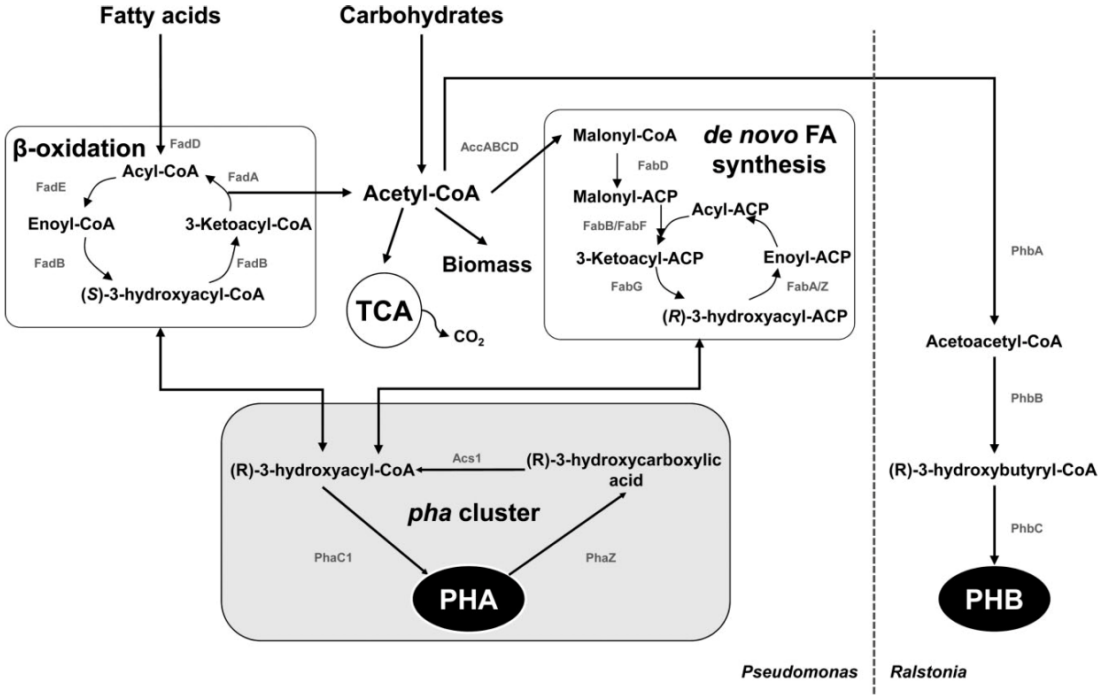

Figure 6. Metabolic pathways involved in PHA biosynthesis of Pseudomonads (left part of the scheme) and PHB in *R. eutropha* (right part of the scheme). The specific PHA/PHB metabolic pathways are interconnected with the main central pathways that converge in acetyl-CoA (Escapa *et al.*, 2012).

The most common PHA is poly-3-hydroxybutyrate (PHB) which is classified as a scl-PHA. In most PHB producing strains, such as the strain *Ralstonia eutropha* H16, the polymer is synthesised through a three-step reaction (De Eugenio *et al.*, 2010). As seen in figure 6 (right side), the reaction starts with acetyl-CoA, more specifically with the condensation reaction of two acetyl-CoA molecules catalysed by a 3-ketothiolase PhbA. Afterwards, the acetoacetyl-CoA molecules formed is stereoselectively reduced to (R)-3-hydroxybutyryl-CoA by a NADPH-dependent acetoacetyl-CoA reductase PhbB. Next, the (R)-3-hydroxybutyryl-CoA monomers are polymerised by a PHB synthase PhbC, releasing CoA.

In the PHB producing bacteria, the intracellular concentrations of acetyl-CoA and free CoA play the central role in regulating the polymer synthesis. A high concentration of acetyl-CoA stimulates the formation of polymers, while a high concentration of free CoA leads to a decrease in the production of PHB. Furthermore, high concentrations of NAD(P)H and high ratios of NAD(P)H/NAD(P) inhibit the citrate synthase activity in the TCA cycle increasing the metabolic flux to the PHB synthesis pathways (Escapa *et al.*, 2012).

Microorganisms that produce mcl-PHAs are less abundant than bacteria that synthesise scl-PHAs. However, it is well known that most Pseudomonads can produce mcl-PHAs, being the *pha* gene cluster responsible for the PHA metabolism conservation within these *Pseudomonas* species. These

microorganisms rely on the β-oxidation pathway and the fatty acid *de novo* synthesis to convert fatty acids or carbohydrate intermediates, respectively, into different (R)-3-hydroxyacyl-CoAs (figure 6). These metabolites serve as substrate for the enzymes that regulate the production of PHAs. The *pha* gene cluster is generally composed of PHA synthesis genes (*phaC1* and *phaC2*), a PHA depolymerase gene (*phaZ*) and the *phaD* gene encoding a putative transcriptional regulator. Some *Pseudomonas* species have additional genes - *phaF* and *phaI* - transcribed divergently from the other *pha* genes that encode phasins. These proteins have regulatory and functional roles in the PHA metabolism. Finally, there is an acyl-CoA synthetase, coded by the gene Acs1, that uses the depolymerase products (3-hydroxyalkanoic acids) and forms the substrates for the polymerases (3-hydroxyacyl-CoAs) via an ATP-dependent reaction (Eugenio *et al.*, 2010).

The knowledge regarding the regulation of PHA biosynthesis in Pseudomonads is still very limited. Little is known about the regulation of production of mcl-PHA at the enzymatic and physiological levels (Escapa *et al.*, 2012). However, it is understood that the molecule 3-hydroxy-acyl-CoA is a common substrate to the PHA pathway and the β-oxidation pathway. Depending on the metabolic state of the cell, the compound is either incorporated into a PHA polymer chain or oxidised via the β-oxidation pathway to make the stored carbon available to the central metabolism. Ren and collaborators, studied in *Pseudomonas putid*a GPo1 how the β-oxidation pathway affected the metabolic flux of the cell to the PHA pathway. The β-oxidation pathway is shown in figure 6. Initially, the fatty acids enter this metabolic pathway by being activated with CoA via the action of an acyl-CoA synthetase encoded by the *fadD* gene. The metabolite formed, acyl-CoA, is then oxidised by an acyl-CoA dehydrogenase and afterwards processed by a protein complex constituted by the acyl-CoA dehydrogenase (*fadE*), enoyl-CoA hydratase (*fadB*), 3-hydroxyacyl-CoA dehydrogenase (*fadB*), cis-Δ^3-trans-Δ^2-enoyl-CoA isomerase, 3-hydroxy-acyl-CoA epimerase, and 3-ketoacyl-CoA thiolase (*fadA*). The molecules NAD and CoA are required for the activity of the enzymes 3-hydroxyacyl-CoA dehydrogenase and 3-ketoacyl thiolase, respectively, controlling the fatty acid oxidation. A low concentration of these metabolites results in an accumulation of 3-hydroxyacyl-CoA and a consequent increase of the metabolic flux to the PHA metabolism pathway (Ren *et al.*, 2009).

1.5. Nile Red for the detection of PHAs

Nile Red is formed by the spontaneous oxidation of Nile blue A in aqueous solution or by refluxing Nile blue with sulfuric acid. This stain is poorly soluble in water but dissolves well in a wide variety of solvents, such as acetone or dimethyl sulfoxide (DMSO). In the presence of organic solvents, Nile Red is strongly fluorescent, but it is quenched in water (Wu *et al.*, 2003). Nile Red was first introduced as a fluorescent stain for intracellular lipids. This compound is photochemically stable, unlike other fluorescent stains like anilionaphathalene sulphate, and its fluorescence capability is strongly dependent on the polarity of its environment. This is why in non-polar solvents, such as hydrocarbon solvents or cholesterol ester droplets, Nile Red becomes fluorescent (Sackett *et al.*, 1987). Therefore, since Nile Red stain is very sensitive to the polarity of the environment, it can be used in different

methods, such as fluorescent microscopy and flow cytofluorometry, to identify strains capable of producing neutral lipids, hydrophobic proteins and PHAs (Zuriani *et al.*, 2013).

1.6. Aim of this work

The objectives behind this project are focused on the investigation of the influence of NADH-dehydrogenases on PHA production in *P. taiwanensis* VLB120. These include the use of different NDHs mutant strains and their characterization in terms of growth behaviour in a minimal medium; applying molecular biology methods to assure no PHA degradation during the experiments; fluorescence microscopy experiments with Nile Red to confirm the presence of PHA granules in the NDHs mutants; and relative quantification procedures to compare the PHA content between the strains to verify the role of NDHs in PHA biosynthesis.

2. Material and Methods

2.1. Chemicals and Enzymes

Chemicals and enzymes were acquired from Carl Roth GmbH & Co. KG (Karlsruhe, Germany), Sigma-Aldrich Chemie GmbH (Steinheim, Germany), Merck KGaA (Darmstadt, Germany) or New England Biolabs GmbH (Frankfurt am Main, Germany).

2.2. Culture media

All the media used in this thesis are described in table 1. When required for the experiments, the antibiotics kanamycin and gentamycin were added to the media, reaching a final concentration of 50 µg/mL and 25 µg/mL, respectively.

Table 1. Culture media used in this thesis.

Medium	Composition
Cetrimide agar	46.7 g/L of cetrimide agar; 1% (v/v) of 100% glycerol; demineralized water.
Delft medium	3.88 g/L of K_2HPO_4; 1.63 g/L of NaH_2PO_4; 2.0 g/L of $(NH_4)_2SO_4$; 10.0 mg/L of EDTA; 0.1 g/L of $MgCl_2.6H_2O$; 2.0 mg/L of $ZnSO_4.7H_2O$; 1.0 mg/L of $CaCl_2.2H_2O$; 5.0 mg/L of $FeSO_4.7H_2O$; 0.20 mg/L of $Na_2MoO_4.2H_2O$; 0.20 mg/L of $CuSO_4.5H_2O$; 0.40 mg/L of $CoCl_2.6H_2O$; 1.0 mg/L of $MnCl_2.2H_2O$; 25 mM of glucose; demineralized water.
Lysogeny broth (LB-medium)	10 g/L of peptone; 5 g/L of yeast extract; 10 g/L of NaCl and 15 g/L of agar in case of the solid medium; demineralised water.
M63 medium	13.6 g/L of KH_2PO_4; 0.2 g/L $(NH4)_2SO_4$; 0.5 mg/L of $FeSO_4.7H_2O$; 15 mM of sodium octanoate; 1 mM of $MgSO_4$; 2.78 mg/L of $FeSO_4.7H2O$; 1.98 mg/L of $MnCl_2.4H_2O$; 2.81 mg/L of $CoSO_4.7H_2O$; 1.47 g/L of $CaCl_2.2H_2O$; 0.17 mg/L of $CuCl_2.2H_2O$; 0.29 mg/L of $ZnSO_4.7H_2O$; demineralized water.

2.3. Microorganisms

Organisms used and created in this thesis are listed in table 2 with their genotype and origin.

Table 2. Strains used in this thesis.

Strain	Genotype	Origin
Escherichia coli DH5α λpir	*endA1*, *glnV44*, *thi-1*, *recA1*, *relA1*, *gyrA96*, *deoR*, *nupG*, *Φ80*, *dlacZ, ΔM15Δ(lacZYA-argF) U169, hsdR17* and λpir phage lysogen	Centro Nacional de Biotecnologia - CSIC, Madrid, Spain
Escherichia coli DH5α λpir pEMG	DH5α λpir + properties of pEMG *	Centro Nacional de Biotecnologia - CSIC, Madrid, Spain
Escherichia coli HB101 pRK2013	HB101 + properties of pRK2013 *	TU Delft, Delft, Netherlands
Escherichia coli DH5α λpir pSW-2	DH5α λpir + properties of pSW-2 *	Centro Nacional de Biotecnologia - CSIC, Madrid, Spain
Pseudomonas taiwanensis VLB120	Wildtype	Biotechnology, TU Dortmund University, Dortmund, Germany
Pseudomonas taiwanensis VLB120*Δ13270*	Wildtype + Knockout of the gene *PVLB_13270*	Institute of Applied Microbiology - iAMB, RWTH-Aachen University, Aachen, Germany
Pseudomonas taiwanensis VLB120*Δ21880*	Wildtype + Knockout of the gene *PVLB_21880*	Institute of Applied Microbiology - iAMB, RWTH-Aachen University, Aachen, Germany
Pseudomonas taiwanensis VLB120*ΔΔndh*	Wildtype + Knockout of the genes *PVLB_13270* and *PVLB_21880*	Institute of Applied Microbiology - iAMB, RWTH-Aachen University, Aachen, Germany
Pseudomonas taiwanensis VLB120*Δnuo*	Wildtype + Knockout of the *nuo* operon (*PVLB_15600-15660*)	Institute of Applied Microbiology - iAMB, RWTH-Aachen University, Aachen, Germany
Pseudomonas taiwanensis VLB120*ΔnuoΔ13270*	Wildtype + Knockout of the *nuo* operon (*PVLB_15600-15660*) and the gene *PVLB_13270*	Institute of Applied Microbiology - iAMB, RWTH-Aachen University, Aachen, Germany
Pseudomonas taiwanensis VLB120*ΔphaZ*	Wildtype + Knockout of the gene *PVLB_02160*	This work

Pseudomonas taiwanensis VLB120*Δ13270ΔphaZ*	*P. taiwanensis* VLB120*Δ13270* + Knockout of the gene *PVLB_02160*	This work
Pseudomonas taiwanensis VLB120*Δ21880ΔphaZ*	*P. taiwanensis* VLB120*Δ21880* + Knockout of the gene *PVLB_02160*	This work
Pseudomonas taiwanensis VLB120*ΔΔndhΔphaZ*	*P. taiwanensis* VLB120*ΔΔndh* + Knockout of the gene *PVLB_02160*	This work
Pseudomonas taiwanensis VLB120*ΔnuoΔphaZ*	*P. taiwanensis* VLB120*Δnuo* + Knockout of the gene *PVLB_02160*	This work
Pseudomonas taiwanensis VLB120*ΔnuoΔ13270ΔphaZ*	*P. taiwanensis* VLB120*ΔnuoΔ13270* + Knockout of the gene *PVLB_02160*	This work
Pseudomonas taiwanensis VLB120*ΔPHA*	Wildtype + Knockout of the PHA operon *PVLB_02159-02161*	Institute of Applied Microbiology - iAMB, RWTH-Aachen University, Aachen, Germany

* The plasmids pEMG, pRK2013 and pSW-2 are described in a following section.

2.4. Growth conditions

2.4.1. *P. taiwanensis* VLB120 cultures

P. taiwanensis VLB120 strains were cultivated in a liquid or solid medium at 30 ºC. The liquid cultures were shaking at 300 rpm in 500 mL pyrex glass flasks (10% of the volume was filled with medium) or in glass pyrex tubes. Pre-cultures were done in glass pyrex tubes with 5 mL of medium and let incubating overnight.

2.4.2. *E. coli* cultures

E. coli strains were grown overnight in liquid LB medium or LB agar plates at 37 ºC. The liquid cultures were shaking at 250 rpm inside glass pyrex tubes.

2.5. Optical density measurement

The optical density of cell suspensions was measured with an Ultrospec 10 Cell Density Meter (Amersham Biosciences, Chalfont St Giles, UK) at an absorbance of 600 nm (OD_{600}). Cell

suspensions samples were diluted to an OD_{600} between 0.02 and 0.6 when the sample reached an OD_{600} higher than 0.6.

2.6. Centrifuges

For the centrifugation of cells or substances inside Eppendorf's of 1.5 or 2 mL the centrifuge Sorvall Legend Micro 17 was used with a rotor of 24x 1.5/2.0 mL containing a click seal biocontainment lid. For the centrifugation of samples inside falcons of 15 or 50 mL, the centrifuge Sorvall Legend X1R was used with the TX-400 swinging bucket rotor carrying the TX-400 rotor adapters with round buckets for 15 or 50 mL falcons. All the centrifuges and adapters are from Thermo Scientific Inc, Karlsruhe, Germany.

2.7. Oligonucleotides

All oligonucleotides used in this thesis were designed using Clone Manager and produced by Eurofins Genomics GmbH (Ebersberg, Germany). Additional regions were added on the primers SN188, SN189, SN190, and SN191 for the Gibson Assembly and were created by the NEBuilder Assembly Tool from New England Biolabs GmbH (Frankfurt am Main, Germany) with a restriction site for the enzyme EcoRI.

Table 3. Oligonucleotides used in this thesis. Additional regions of the primers are in bold.

Primer	Sequence (5´ → 3´)	Comment
SN188	**AGGGATAACAGGGTAATCTG**GCGACCTCATCGAGATGTTC	fwd TS1
SN189	**GAGCGCAGCG**GCGCGTGACTCTGTGGTGAAAG	rev TS1
SN190	**AGTCACGCGC**CGCTGCGCTCTTGTTTGTACG	fwd TS2
SN191	**ATCCCCGGGTACCGAGCTCG**GGCTTTGGCCGCCAGTATTG	rev TS2
SN192	ACTACCTGCTGGGCAACGAG	verification fwd
SN193	CTCATTGCGAAACACCACTG	verification rev
BW013	TTTGCACTGCCGGTAGAAC	fwd pEMG
BW014	AATACGCAAACCGCCTCTC	rev pEMG
SN027	ATACGGGCCGTTCATCAGTC	fwd *Δ13270*
SN028	GCGATCTTGCGAATGGTGTC	rev *Δ13270*
SN029	CCGGCTGAATGACGAATG	fwd *Δ21880*

SN030	GTTACGACCCGGTGTATG	rev *Δ21880*
SN116	CTCGTCCAAGCCACCTGATG	fwd *Δnuo*
SN117	AGCCTCAAGGTCATGGTCTG	rev *Δnuo* del
SN171	CGGACACAGACCATGCATAC	rev *Δnuo* wt

2.8. Production of competent *E. coli* DH5α λpir cells

Competent *E. coli* cells were prepared according to Hanahan and collaborators (Hanahan *et al*., 1983). The procedure started with 0.2 mL of an overnight culture of *E. coli* DH5α λpir cells to inoculate 5 mL of liquid LB-medium. When the culture reached an OD_{600} of 0.3, the cell suspension was collected to a falcon and rested in ice for 10 minutes. Next, the cells were centrifuged at 4,500 rpm at 4 °C for 15 minutes. The supernatant was discarded and the cells resuspended in 10 mL of sterile 0.1 M $CaCl_2$ solution. Afterwards, the falcon was placed on ice for 30 minutes and centrifuged again at 4,500 rpm at 4 °C for 15 minutes. The supernatant was discarded and the pellet resuspended in 3 mL of 0.1 M $CaCl_2$ and 1 mL of sterile 50% glycerol. The competent cells were then stored as 0.2 mL aliquots at -80 °C.

2.9. Plasmid isolation from *E. coli* strains

Plasmid isolation from *E. coli* strains was done using AIAprep Spin Miniprep Kit (Qiagen, Hilden, Germany). The procedure was carried out according to the instruction manual of the manufacturer.

2.10. Isolation of genomic DNA from *P. taiwanensis* VLB120 strains

Genomic DNA isolation from *P. taiwanensis* VLB120 strains was achieved by using the AIAprep Spin Miniprep Kit from Qiagen (Hilden, Germany). The procedure was carried out according to the instruction manual of the manufacturer.

2.11. Polymerase chain reaction (PCR)

The PCR conductions were conducted in the FlexCycler (Analytik Jena AG, Jena, Germany). The polymerases used were Q5® High-Fidelity DNA polymerase and OneTaq® DNA polymerase with 2x master mix and standard buffer. Both polymerases are from New England Biolabs GmbH (Frankfurt am Main, Germany). The programs used in the FlexCycler for these enzymes are represented in table 4 and table 5.

PCR reactions using the Q5® High-Fidelity DNA polymerase were carried out in 50 μL reactions and PCR reactions using the OneTaq® DNA polymerase were done in 20 μL reactions. The

components used in the PCR reactions for both DNA polymerases are described in table 6 and table 7.

Table 4. PCR program for the DNA polymerase Q5® High-Fidelity.

PCR steps	Temperature (º C)	Time (min:s)
1	98	00:30
2	98	00:10
3	T_m	00:30
4	72	t_e
5	72	02:00
6	10	Pause

* The steps between 2 and 4 were repeated thirty times.

Table 5. PCR program for the DNA polymerase OneTaq®

PCR steps	Temperature (º C)	Time (min:s)
1	94	10:00
2	94	00:30
3	T_m	00:30
4	68	t_e
5	68	05:00
6	10	Pause

* The steps between 2 and 4 were repeated twenty-five times.

Table 6. Components of one 20 μL PCR reaction using the DNA polymerase OneTaq®

Component	20 μL reaction
Master mix green Taq (1x)	10 μL
Lysate	1 μL
10 μM forward primer	0.5 μL
10 μM reverse primer	0.5 μL
Nuclease-free water	8 μL

Table 7. Components of one 50 μL PCR reaction using the DNA polymerase Q5® High-Fidelity.

Component	50 μL reaction	Final concentration
5x Q5 reaction buffer	10 μL	1x
10 mM dNTPs	1 μL	200 μM
10 μM forward primer	2.5 μL	0.5 μM
10 μM reverse primer	2.5 μL	0.5 μM
Template DNA	0.5 μL	<1000 ng
Q5 DNA polymerase	0.5 μL	0.02 U/μL
5x Q5 enhancer	10 μL	1X
Nuclease-free water	To 50 μL	-

2.12. Purification of PCR products

PCR product purification was done by using the GenepHlow™ Gel/PCR kit from Geneaid Ltd (Taiwan). The procedure was carried out according to the instruction manual of the manufacturer.

2.13. Agarose gel electrophoresis

DNA fragments were separated and observed with 1% (w/v) agarose gels in TAE buffer (40 mM Tris, 2 mM EDTA, pH 8). For staining, 1 μL of Roti®-Safe GelStain from Carl Roth GmbH & Co. KG (Karlsruhe, Germany) was added to each 20 mL of 1% (w/v) agarose solution prepared. To estimate the size of the DNA fragments, the gene ruler 1 kb DNA ladder from Sigma-Aldrich Chemie GmbH (Steinheim, Germany) was used.

2.14. Determination of DNA concentration

The concentration of double-stranded DNA was determined using NanoDrop One (Thermo Scientific Inc., Karlsruhe, Germany). The concentration was measured at an absorbance of 260 nm.

2.15. Plasmids

2.15.1. Plasmid pEMG

The most relevant features present on the pEMG plasmid (figure 7) consist on a multiple cloning site (MCS), flanked by I-SceI sites, engineered within a *lacZα* operon, a kanamycin resistance cassette (Km^R), and the components necessary for conjugative mobilization, origin of transfer (*oril*) and transfer gene (*traJ*). Furthermore, it also includes an origin of replication, *ori*R6K that is dependent on the protein pi.

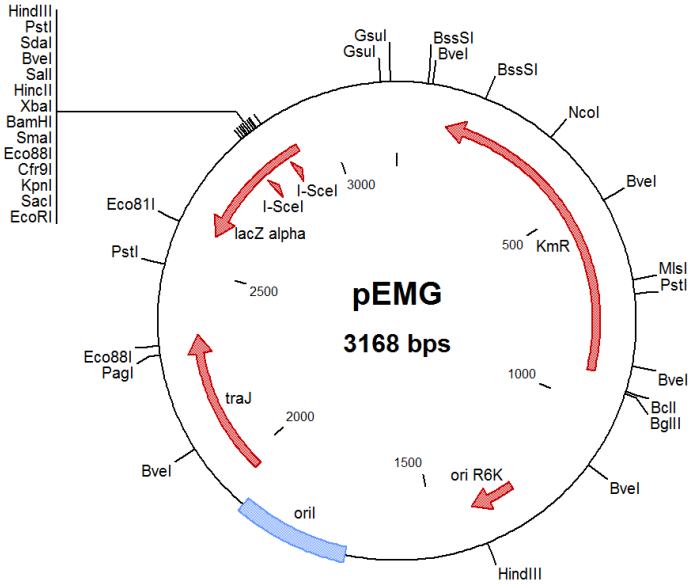

Figure 7. pEMG plasmid map. KmR: kanamycin resistance cassette; lacZα: *lacZ* operon; oriR6K: narrow host range of replication dependent on the protein pi; oriI: an origin of transfer; traJ: transfer genes.

2.15.2. Plasmid pSW-2

The plasmid pSW-2 contains a gentamycin resistance cassette (Gm^R), a broad host origin of replication (*ori*RK2), genes coding for the TrfA proteins (*trfA*) and an origin of transfer (*oriT*). This plasmid expresses the I-SecI nuclease upon the activation of the *Pm* promoter that is dependent on the XylS protein. The gene coding for the regulatory proteins is also present in the plasmid. A transcriptional terminator (T) is located downstream of the I-SceI gene.

2.15.3. Plasmid pRK2013

The conjugative plasmid pRK2013 contains a kanamycin resistance cassette (Km^R), a narrow host origin of replication (*oriCoIE1*) and the *tra* and *mob* genes.

2.16. Tri-parental mating

Tri-parental mating was the method used to transfer the necessary plasmids for the knockout of the PHA depolymerase gene in the *Pseudomonas* strains. *E. coli* DH5α λpir with the pEMG construct or the pSW-2 plasmid, depending on the phase of the gene knockout protocol, were used as the donor strains; *E. coli* HB101 pRK2013 the helper strain; and the *P. taiwanensis* VLB120 NADH-dehydrogenases mutant strains the recipients. Genetic material was transferred between strains by streaking out an inoculation loop of each strain on top of each other on a non-selective LB-medium plate and incubated overnight at 30 ºC. A loop of the mating lawn was then streaked out in cetrimide agar plates supplemented with the kanamycin or gentamycin depending on the selection need it.

2.17. pEMG vector enzymatic digestion

pEMG vector was linearized with the high-fidelity restriction enzyme EcoRI-HF® from New England Biolabs GmbH (Frankfurt am Main, Germany).

2.18. Gibson Assembly of the pEMG-TS1/TS2

A Gibson assembly construct was created by using the Gibson Assembly™ Cloning Kit from New England Biolabs GmbH (Frankfurt am Main, Germany).

2.19. Transformation of *E. coli* DH5α λpir cells with the pEMG construct

Transformation of the *E. coli* DH5α λpir cells with the product plasmid was carried out according to the protocol described in New England BioLabs. Initially, 100 µL of competent cells were thawed on ice for 15 minutes. Then, 2 µL of the chilled assembly product was added and mixed by gently flicking the tube. The mixture was placed on ice for 30 minutes, subsequently submitted to a heat shock of 42 °C for 30 seconds and then put on ice again for 2 minutes. 950 µL of room temperature LB-medium was added to the tube and incubated at 37 °C shaking at 250 rpm for 60 minutes. Afterwards, 100 µL of the cells were spread on selection plates of LB medium and kanamycin that were preheated beforehand at 37 °C. The cells were then incubated at 37 °C overnight.

2.20. Colony PCR with alkaline poly(ethylene glycol) (PEG)

The colony PCR procedure was based on the work of Chomczynski and collaborators (Chomczynski *et al.*, 2006). An alkaline PEG solution to lyse the cells was prepared by combining 60 g of PEG 200 with 0.93 mL of 2 M KOH and 39 mL of water. Cell material taken from a colony was put in a PCR tube with 50 µL of alkaline reagent and let incubating for 10 minutes. 20 µL PCR reactions were done with 1 µL of lysate used.

2.21. PHA depolymerase gene knockout via homologous recombination

E. coli DH5α λpir colonies with the pEMG construct were obtained after screening the selection plates for positive clones. Afterwards, the colonies selected were platted in a master plate with LB medium and kanamycin and left growing overnight. The verification of the presence of the construct in the *E. coli* cells was done by submitting individual colonies to a colony PCR. A positive clone was then platted in a LB medium and kanamycin plate, left growing overnight and then used in a tri-parental mating to transfer the pEMG construct to the desired *P. taiwanensis* VLB120 mutant strain. Single colonies obtained from the streaked out of the mating lawn were then platted in a cetrimide agar and kanamycin master plate. Colony PCRs were then used to verify the correct integration of the construct. Finished this procedure, the co-integrate clone received the pSW-2 plasmid again via tri-parental mating. However, in this phase of the experimental work the cetrimide agar plates were supplemented with gentamycin to select the clones that received the pSW-2 plasmid. Single colonies,

obtained from the previous step, were streaked out on LB and gentamicin plates and LB and kanamycin plates in the same positions. The colonies that were kanamycin sensitive were the cells of interest because they suffered recombination and lost the gene of interest or reverted to the wildtype strain. The clones of interest are retrieved from the LB and gentamycin plates. After this, a screening was done with colony PCRs to verify if the desired knockout was achieved. The *Pseudomonas* cells lost the pSW-2 plasmid after streaking out several generations on a non-selective medium (LB-medium) and testing for gentamycin sensitivity in LB and gentamycin plates. Colonies were sent to sequencing to confirm the knockout of the desired gene. After the sequencing confirmation, cryocultures of the PHA depolymerase mutant strains were prepared.

2.22. Sequencing

Sequencing of DNA fragments was done by Eurofins MWG Operon (Ebersberg, Germany).

2.23. Cryocultures

Cryocultures were done by adding 300 µL of glycerol to 700 µL of overnight cultures of *Pseudomonas taiwanensis* VLB120 PHA depolymerase mutant strains. The aliquots were then vortexed and stored at -80 ^{o}C.

2.24. Nile Red staining

PHAs of the *Pseudomonas* strains were stained using the compound Nile Red. A stock solution of this substance was prepared by solving Nile Red in dimethyl sulfoxide (DMSO) resulting in a final concentration of 80 µg/mL. The staining procedure depends on the experiment being conducted.

2.24.1. Staining of PHAs for fluorescence microscopy

Samples from the cell cultures were collected and normalised to 1 mL with an OD_{600} of 2.5. Then the samples were centrifuged for 2 minutes at 13,300 rpm and the resulting pellet resuspended in 100 µL of 0.9% NaCl solution. Afterwards, 90 µL of the sample was transferred to an Eppendorf tube and 10 µL of Nile Red was added. The mixture was vortexed and incubated in the dark for 30 minutes.

2.24.2. Staining of PHAs for fluorescence intensity measurement

The staining method was carried out according to Zuriani and collaborators (Zuriani *et al*. 2013). After collecting samples from the cells cultures and measure their OD_{600}, 800 µL of cell culture was transferred to a 1.5 mL Eppendorf tube and centrifuged at 14,000 rpm for 3 minutes. The pellet was then resuspended in 800 µL of 0.9% NaCl and normalised to a volume of 350 µL with an OD_{600} of 0.3. Subsequently, 14 µL of the Nile Red stock solution was added to the cell suspension, vortexed and incubated in the dark at room temperature for 30 minutes.

2.25. Fluorescence microscopy

The Nile red fluorescence present in the cells was observed using the fluorescence microscope Leica DM6000 B (Wetzlar, Germany). The fluorescence was read at an excitation and emission wavelength of 515 and 590 nm, respectively. It was used a lens with a magnification x63 with oil immersion. The settings used in the Leica AF6000 Modular Systems for image acquisition were an exposure time, gain, and intensity of 346.15 ms, 1 and 2, respectively.

2.26. Fluorescence intensity measurement

Nile Red fluorescence intensity was measured with a Synergy Mx microplate reader (BioTek Instruments Inc., Winooski, USA). To read the samples with this device, 100 µL of cell cultures were transferred to a Microfluor 1Black 96 wells flat bottom microtiter plates (Thermo Scientific, New York, USA). The program Gen5 was used for data collection and analysis. The settings introduced in the program for the Nile Red fluorescence measurement was based on Zuriani and collaborators (Zuriani *et al*., 2013). The excitation and emission wavelength used were 535 and 605 nm, respectively. The gain was defined to 100.

2.27. Sample preparation for GC-MS analysis of PHAs

The sample preparation for GC-MS analysis of PHAs was conducted as described in the work of Schmitz and collaborators (Schmitz *et al.*, 2015). When the cell cultures reached the stationary phase, the samples were collected in 50 mL falcons and centrifuged at 7,000 rpm for 7 minutes. The pellet was washed with a 0.9% NaCl solution and lyophilized overnight in a ScanVac CoolSafe freeze dryer from LaboGene (Lillerød, Deenmark) with a chamber capacity of 9 L.

PHA extraction from the dried cells was conducted through a methanolysis process. Per 10 mg of dry cell weight, 2 mL of chloroform and 2 mL of methanol containing 15% sulfuric acid and 0.5 mg/mL of benzoic acid, as an internal standard (IS), was added and incubated at 100 ºC for 4 hours.

Then, a derivatization process was done by mixing 30 µL of N-methyl-N-(trimethylsilyl) trifluoroacetamide (MSTFA) with 30 µL of a methanolysed organic sample at 85 ºC for 1 hour.

The final structure of the PHA monomers, after methanolysis and derivatisation with MSTFA, is represented in figure 8.

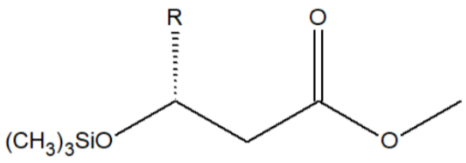

Figure 8. PHA structure after methanolysis and derivatization with MSTFA. Adapted from the work of Klinke and colleagues (Klinke *et al*, 1999).

2.28. GC-MS analysis for PHA identification and content determination

Qualitative quantification and identification of PHAs were achieved by using gas chromatography (Trace GC Ultra, Thermo Scientific) coupled to a mass spectrum analysis (TSQ 8000, Triple Quadrupole MS, Thermo Scientific).

An aliquot of 1 µL of derivatized sample was injected into the gas chromatograph at a split ratio of 1:50. Separation of the compounds was done using a VF-5ms column from Agilent J&W GC Columns that has 5% phenylmethyl, 30 meters in length, 0.25 mm in diameter and 0.25 µm of film thickness. The carrier gas was helium at a flow rate of 0.9 mL/min. The injector and transfer line temperature was established to 275 ºC and 290 ºC, respectively. The oven temperature program was: an initial temperature of 80 ºC for 2 minutes, following an increment from 80 ºC to 150 ºC at a rate of 5 ºC/min and then up to 200 ºC at a rate of 10 ºC/min. The electron ionization (EI) mass spectrum was recorded in full scan mode - m/z 40-550.

3. Results

The results of this thesis are divided into five main sections: growth characterization of NADH-dehydrogenase mutant strains in minimal medium; knockout of the PHA depolymerase gene to assure no PHA degradation; fluorescence microscopy with Nile Red to visualize PHA granules; and relative quantification of the PHA content inside the cells using two different methods, Nile Red rapid method and GC-MS.

3.1. Growth characterization of NADH-dehydrogenase mutant strains

The different NADH-dehydrogenases mutant strains used in this project can be seen in table 8. These mutants were already available in the laboratory, but no further characterization had been performed. Therefore, a growth characterization of the strains was conducted to verify if the NDH mutations affected the metabolism of the cells. Thus, the working strains were inoculated in Delft medium with an initial OD_{600} of 0.1. Overnight cultures of the respective strains were used to inoculate the flasks. After two hours of incubation, the OD_{600} of the cultures was measured every 30 or 60 minutes. After the lag phase of two hours, the next samples were measured every 30 minutes to capture the beginning of the exponential phase. Afterwards, the OD_{600} was measured every 60 minutes until the optical density of the cultures did not deviate significantly.

Table 8. *P. taiwanensis* VLB120 NADH-dehydrogenase deficient strains generated through homologous recombination. The strain *P. taiwanensis* VLB120*ΔnuoΔ21880* was not generated.

	NADH-dehydrogenase type I	**NADH-dehydrogenase type II**	
	Nuo-complex	***PVLB_13270***	***PVLB_21880***
Wildtype/reference	active	active	active
Δ13270	active	x	active
Δ21880	active	active	x
ΔΔndh	active	x	x
Δnuo	x	active	active
ΔnuoΔ13270	x	x	active

The growth curves of all the strains can be observed in figure 9. As expected, the cultures presented the normal phases, more specifically the lag phase in the beginning, followed by the exponential phase and the stationary phase. Furthermore, a diauxic behaviour seems to be presence in some of the curves, like for example in the strain *P. taiwanensis* VLB120 after 4.5 hours of growth.

All the mutant strains had a growth behavior similar to the wildtype, except the strain *P. taiwanensis* VLB120*ΔΔndh* that got its metabolism affected by the NDHs mutations. In the stationary phase, strain *P. taiwanensis* VLB120*ΔΔndh* reached a maximum OD_{600} of 3.8, while the other strains oscillated between 4.9 and 5.3 (supplemental data, S1).

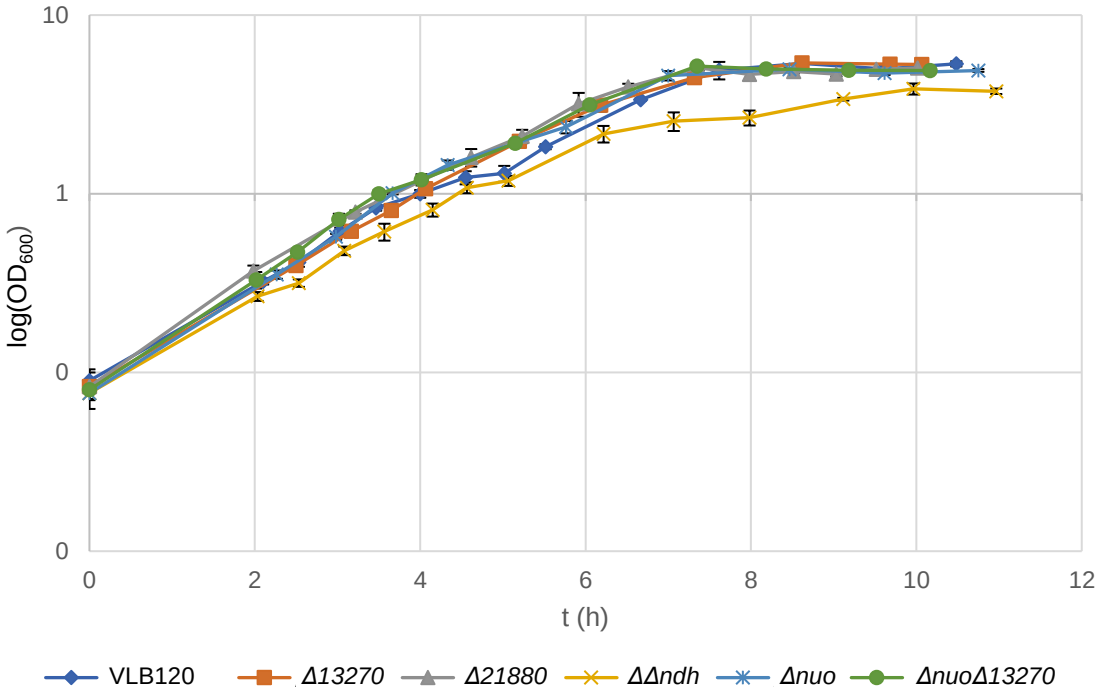

Figure 9. Growth curve experiments of *P. taiwanensis* VLB120, *P. taiwanensis* VLB120*Δ13270*, *P. taiwanensis* VLB120*Δ21880*, *P. taiwanensis* VLB120*ΔΔndh*, *P. taiwanensis* VLB120*Δnuo* and *P. taiwanensis* VLB120*ΔnuoΔ13270*, represented in logarithm scale. The *Pseudomonas* strains were cultivated in minimal medium (Delft), with 25 mM of glucose, at 30 ºC at a shaking velocity of 300 rpm.

3.2. Knockout of the PHA depolymerase encoding gene

After observing the effect of the NDHs mutations on growth behavior of the strain *P. taiwanensis* VLB120, the knockout of the PHA depolymerase gene, *PVLB_02160*, was conducted by homologous recombination using the pEMG vector system (Martínez *et. al,* 2011).

The *P. taiwanensis* VLB120 strains produce PHAs when there is an environmental stress and excess of carbon in the medium, as explained in the section 1.3. Considering the aim of the project, the cells were cultivated in a minimal medium that would not stimulate the syntheses of the polymer, allowing to see only the influence of the NDHs in PHA production. However, it is known that if PHA granules are accumulated in the cytoplasm and the environmental stress, that induced the production of PHAs, is lifted, the cells will start consuming the PHAs (Ren *et al.*, 2009). Thus, there was the possibility that if the mutants produced PHA's, due to the NDHs mutations, they would consume it immediately. This was the reason for the realization of the knockout of the PHA depolymerase gene - to guarantee no PHA degradation in the following experiments.

3.2.1.Assembly of the pEMG-TS1/TS2 construct

To accomplish this genomic modification, the downstream and upstream regions of the target gene (TS1 and TS2) were amplified via PCR, using, respectively, the primers SN188/SN189 and SN190/SN191 and as template the isolated genome of *P. taiwanensis* VLB120. The amplification of TS1 and TS2 regions was done under the same PCR conditions. Q5® High-Fidelity DNA polymerase was used with an annealing temperature of 68 ºC and an elongation time of 15 seconds. The PCR products TS1 and TS2 presented approximately a size of 515 bp and 522 bp, respectively, as predicted and those results can be observed on figure 10 (lanes #3 and #4 for TS1 and lanes #5 and #6 for TS2). The plasmid pEMG was linearized with the restriction enzyme EcoRI-HF. As expected, the linear plasmid (figure 10, lane #2) was about 3168 bp and the circular plasmid (figure 10, lane #1) had a band with more than 10,000 bp.

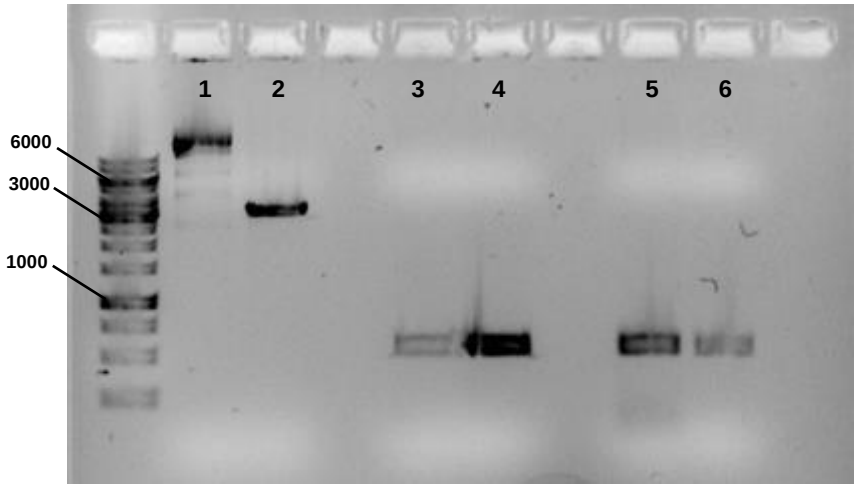

Figure 10. Agarose gel electrophoresis with several fragments used in the Gibson assembly: circular plasmid pEMG (#1), plasmid pEMG digested (#2), impure TS1 fragments (#3), purified TS1 fragments (#4), impure TS2 fragments (#5) and purified TS2 fragments (#6). In the first lane is present the gene ruler 1 kb DNA ladder (Fermentas) with indicated sizes in base pairs.

The assemble of the three fragments was conducted as described in the Gibson Assembly™ Cloning Kit from New England Biolabs GmbH (Frankfurt am Main, Germany). After the assembly, the construct was chemically transformed into *E. coli* DH5α *λ*pir cells, which were than streaked out in LB plates supplemented with kanamycin. Afterwards, thirty positive clones were selected and streaked out in a master plate. After growing overnight, the colonies were submitted to a colony PCR, to verify the insertion of the regions TS1 and TS2 into the pEMG plasmid. The PCR was conducted using the primers BW013 and BW014, an annealing temperature of 53 ºC and an elongation time of 1.8 minutes. As expected, colonies with the Gibson assembly construct had a band approximately with 1596 bps, although colonies with just the pEMG plasmid had a band with about 559 bps. In figure 11, colonies with the correct construct are seen (for example in lanes #1 and #2) and the empty pEMG vector is in lane #8.

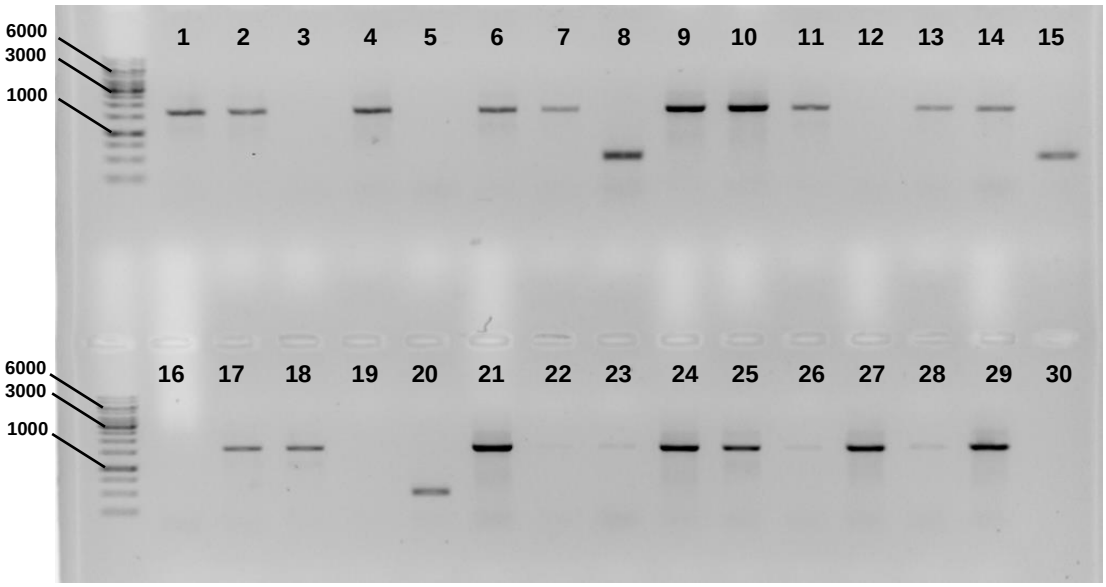

Figure 11. Verification of construct pEMG – TS1/TS2 through colony PCR of thirty *E. coli* DH5α *λ*pir colonies. The PCR results have amongst them a fragment with a size of approximately 1596 bp, if the regions TS1 and TS2 are inserted in the plasmid, and a fragment of about 559 bp, if it is the empty pEMG plasmid. In the first lane is present the gene ruler 1 kb DNA ladder (Fermentas) with indicated sizes in base pairs.

3.2.2. Integration of the pEMG-TS1/TS2 construct into *P. taiwanensis* VLB120 genome

After cloning the homologous regions, TS1 and TS2, into the pEMG plasmid, tri-parental mating was used to transfer the construct to the cells of the NADH-dehydrogenases mutant strains. The integration of the construct into the genome of the working strains was confirmed by colony PCR, using two different sets of primers, SN192/BW014 and BW013/SN193 (figure 12). With these two sets of primers, the direction of the integrated plasmid in the genome can be known. For both PCR reactions, the OneTaq polymerase was used with the 2x standard buffer and with an elongation time of 2.5 minutes. Furthermore, the set of primers SN192/BW014 and BW013/SN193 used an annealing temperature of 53 ºC and 52 ºC, respectively.

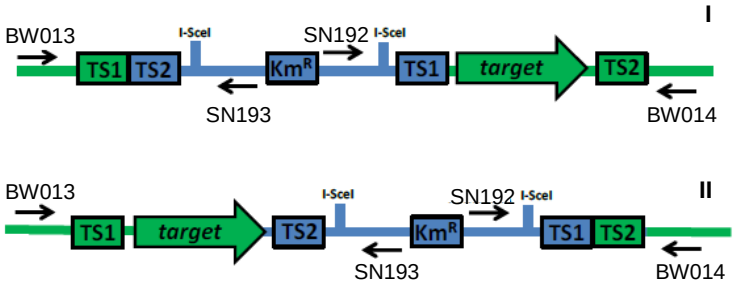

Figure 12. The two possible directions which the plasmid can integrate the genome of *P. taiwanensis* VLB120.

As an example, PCR results of the integration of the construct into the genome of *P. taiwanensis* VLB120*Δnuo* are shown in figure 13. As expected, when the plasmid integrates the genome in the position I the primers SN192/BW014 originated a band with approximately 2282 bp and the primers BW013/SN193 a band with about 1427 bp. However, when integrated into the position II the set of

primers SN192/BW014 originated a DNA fragment with approximately 1424 bp and the primers BW013/SN193 a band with about 2285 bp.

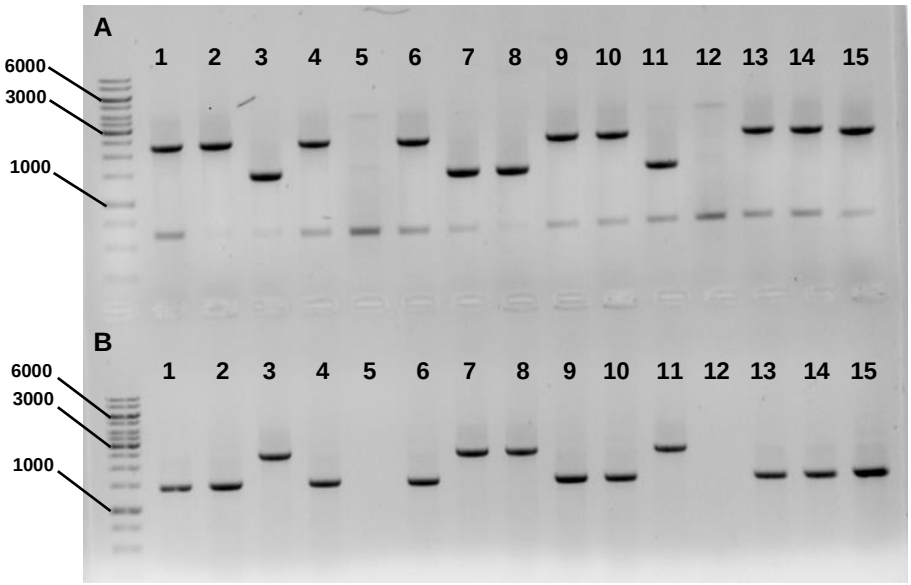

Figure 13. Confirmation of the insertion of construct pEMG – TS1/TS2 into the genome of strain *P. taiwanensis* VLB120Δ*nuo*. (**A**) colonies were submitted to colony PCRs with the primers SN192 and BW014 and (**B**) colony PCRs were conducted using the primers BW013 and SN193. Fifteen different colonies were used. In the first lane is present the gene ruler 1 kb DNA ladder (Fermentas) with indicated sizes in base pairs.

3.2.3. Deletion of the PHA depolymerase gene

Next, the pSW-2 plasmid was transferred to the recipient strains by tri-parental mating. Gentamicin resistant colonies from the previous step were submitted to colony PCRs to verify the knockout of the PHA depolymerase gene, *PVLB_02160*. The PCRs reactions were conducted using the set of primers SN192/SN193 with an annealing temperature of 52 ºC and an elongation time of 2.20 minutes. As expected, some colonies originated a band with a size of about 2113 bp, corresponding to the wildtype genome, or a band with a size near 1255 bp that indicates the deletion of the target gene. For example, in figure 14 it can be observed colonies from the strain *P. taiwanensis* VLB120*Δnuo* with bands corresponding to the size mentioned.

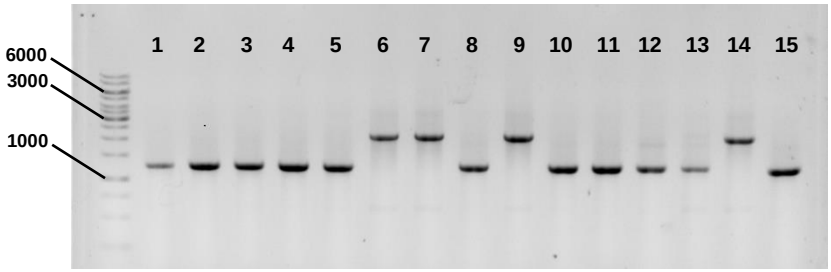

Figure 14. Confirmation of the knockout of the target gene in strain *P. taiwanensis* VLB120*Δnuo*. Fifteen different colonies were used. In the first lane of the agarose gel is present the gene ruler 1 kb DNA ladder (Fermentas) with indicated sizes in base pairs.

Afterwards, five positive colonies from each strain were selected, and the colony PCR redone to assure that the colonies selected from the master plate had the knockout of the desired gene (figure 15).

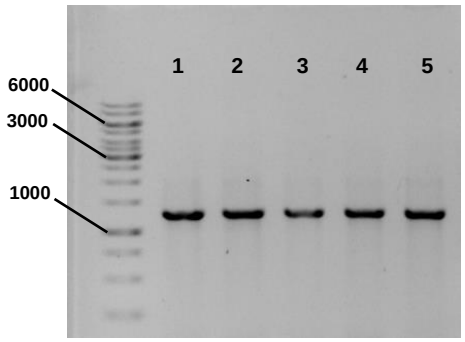

Figure 15. Confirmation of the genotype of mutant strains of *P. taiwanensis* VLB120*ΔnuoΔphaZ* by colony PCR. Five colonies were used. In the first lane of the agarose gel is present the gene ruler 1 kb DNA ladder (Fermentas) with indicated sizes in base pairs.

The results from all five colonies showed the presence of a band with the size of approximately 1255 bp. One PCR reaction from each strain was purified and sent for sequencing. All the sequencing results indicated high homology between the genome of the working strains and the genomic model created in Clone manager for the PHA operon in *P. taiwanensis* VLB120 without the PHA depolymerase gene. Afterwards, cryocultures of the PHA depolymerase mutant strains were done. From this point on, all the experiments were conducted with the strains with the knockout of the PHA depolymerase gene *phaZ*.

3.2.4. Verification of the NDHs mutants

To confirm if there was no mix between the NDHs mutant strains during the knockout of the *phaz* gene, colony PCRs were performed to all working strains. The presence of the genes encoding the complex I (*nuo* operon) and the NDHs-II (*PVLB_13270* and *PVLB_21880*) was tested in all the working strains.

The presence of the *nuo* operon was checked using two sets of primers, but three different primers (SN116, SN117 and SN171). The set of primers SN116/SN117 were used to verify the deletion of the operon. These two primers bind to the genome, flanking the operon. The pair of primers SN116/SN171 allows the confirmation of the presence of the *nuo* complex, since the primer SN171 binds in the beginning of the operon. The pair of primers SN116/SN117 was used with an annealing temperature of 55 ºC, an elongation time of 2.1 minutes and, if the *nuo* operon was deleted, originates a PCR fragment nearly with 1955 bp. The set of primers SN116/SN171 were used with an annealing temperature of 54 ºC, an elongation time of 1.5 minutes, and, if the *nuo* operon is present, originates a PCR product of about 1311 bp.

To confirm the presence of the gene *PVLB_13270* the set of primers SN027 and SN28 were used in the colony PCR, with an annealing temperature of 55 ºC and an elongation time of 3.5 minutes. In

the presence of the gene, the PCR product originated should have a size close to 3346 bp. Otherwise, if it is the knockout strain, the PCR fragment should be around 2059 bp. The primers annealed in the genome of the Pseudomonads just before and after the gene.

In the case of the gene *PVLB_21880*, the set of primers SN029 and SN030 were used in the colony PCR with an annealing temperature of 50 ºC and an elongation time of 3.1 minutes. A PCR fragment is originated with a size near 2997 bps if the gene is present. If the gene is deleted the size of the product is approximately 1633 bp. Like in the confirmation of the other NDH-II gene, the primers annealed, flanking the target gene.

The results presented in figure 16 show that there was no mix between the strains. However, for some unknown reason, no bands appeared in the electrophoresis gel for the verification of the gene *PVLB_21880* in the strain *P. taiwanensis* VLB120*Δ13270ΔphaZ* (upper right corner of figure 16). For this reason, the verification of the NDH-II genes was repeated for the strain *P. taiwanensis* VLB120*Δ13270ΔphaZ* (figure 17).

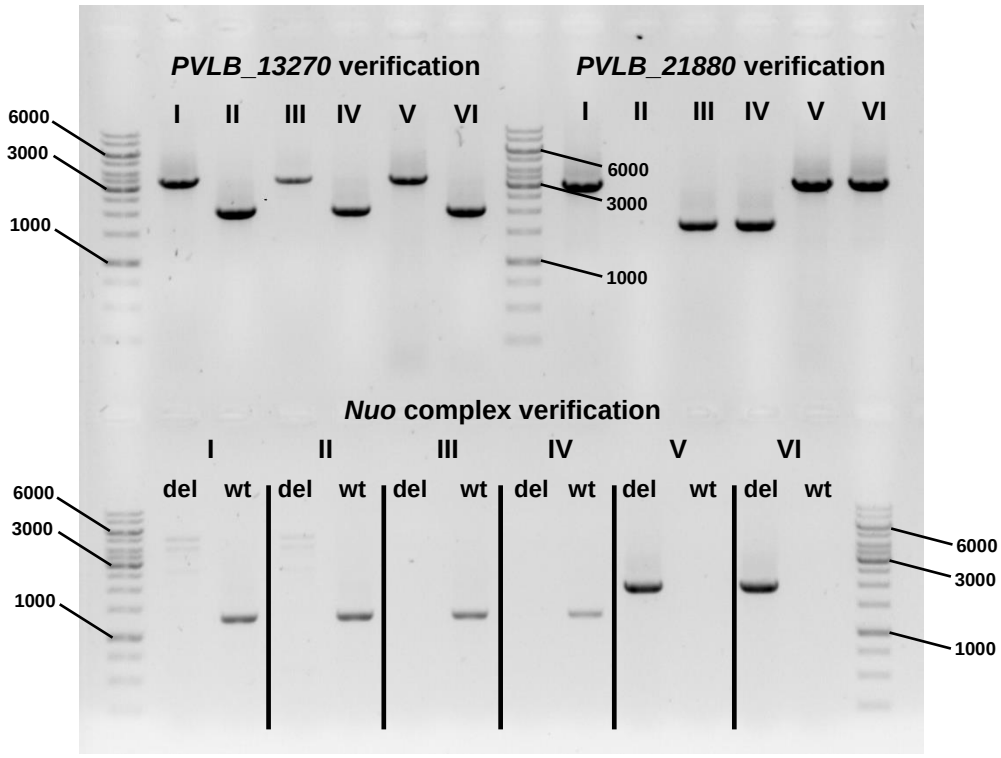

Figure 16. Confirmation of the NADH-dehydrogenases strains after the *phaZ* gene knockout. The numbers I, II, III, IV, V and VI represent the strains *P. taiwanensis* VLB120*ΔphaZ*, *P. taiwanensis* VLB120*Δ13270ΔphaZ, P. taiwanensis* VLB120*Δ21880ΔphaZ*, *P. taiwanensis* VLB120*ΔΔndhΔphaZ*, *P. taiwanensis* VLB120*ΔnuoΔphaZ* and *P. taiwanensis* VLB120*ΔnuoΔ13270ΔphaZ*, respectively. The verification of the deletion of the *PVLB_13270* gene was confirmed using the set of primers SN027/ SN028 and the results are represented on the top left part of the image. The verification of the deletion of the *PVLB_21880* gene was done with set of primers SN029 and SN030 and results are represented on the top right of the image. In relation to the *nuo* complex two sets of primers were used (results in the bottom of the image). The primers SN116 and SN117 were used to verify if the complex was deleted (lanes labelled “del”) and the primers SN116 and SN171 to verify if the *nuo* complex was present (lanes labelled “wt”). It was used the gene ruler 1 kb DNA ladder (Fermentas) with indicated sizes in base pairs.

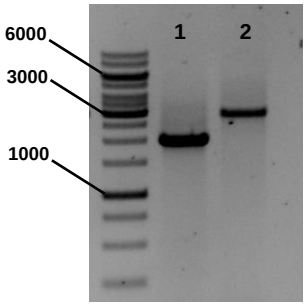

Figure 17. Confirmation of the NADH-dehydrogenase *P. taiwanensis* VLB120*Δ13270ΔphaZ* strain. In position 1 the deletion of the gene *PVLB_13270* was verified with the primers SN027/SN028 and in position 2 the deletion of the gene *PVLB_21880* was checked with the primers SN029/SN030. It was used the gene ruler 1 kb DNA ladder (Fermentas) with indicated sizes in base pairs.

3.3. Fluorescence microscopy

After knocking out the PHA depolymerase gene, cells from three working strains were observed under a fluoresce microscope with the intent of detecting PHA granules in the NDHs mutants. The strains *P. taiwanensis* VLB120*ΔnuoΔphaZ*, *P. taiwanensis* VLB120*ΔphaZ* and *P. taiwanensis* VLB120 were cultivated in Delft medium and, after a period of twenty-four hours, the cells were stained with Nile Red and observed under the fluorescence microscope. The strain *P. taiwanensis* VLB120*ΔPHA* was used as control since does not produce PHAs.

The cells from strains *P. taiwanensis* VLB120*ΔphaZ* and *P. taiwanensis* VLB120*ΔPHA* have a similar morphology (figure 18 IA and IB), but strain *P. taiwanensis* VLB120*ΔnuoΔphaZ* has a longer rod shape (figure 18 IC) than the other strains. The fluorescence microscopy experiments allow to verify the presence of PHA granules in the NDH mutants. All the strains showed red fluorescence, but only in the strains, *P. taiwanensis* VLB120*ΔphaZ* and *P. taiwanensis* VLB120*ΔnuoΔphaZ* PHA granules can be observed (figure 18 IIB and IIC). Cells from the strain *P. taiwanensis* VLB120*ΔnuoΔphaZ* had more PHA granules when compared to *P. taiwanensis* VLB120*ΔphaZ*, hinting for the influence of the NDHs in PHA production.

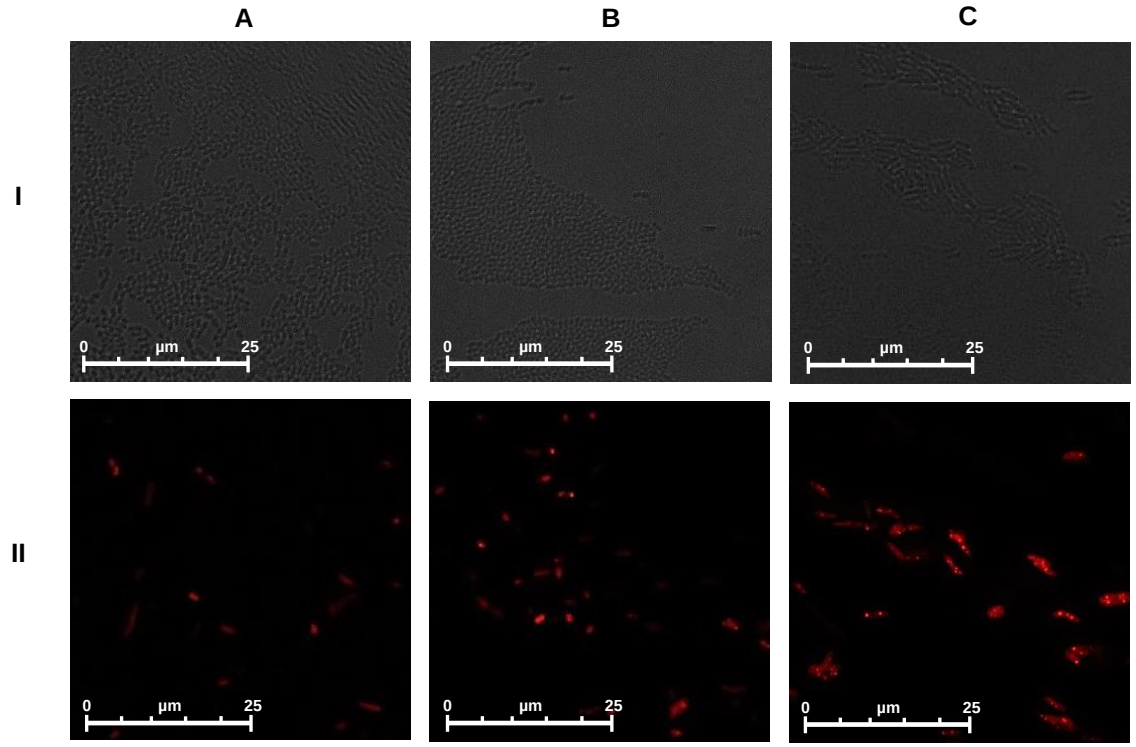

Figure 18. Phase contrast images (**I**) and fluorescence microscopy images (**II**) of *P. taiwanensis* VLB120*ΔPHA* **(A)**, *P. taiwanensis* VLB120*ΔphaZ* **(B)** and *P. taiwanensis* VLB120*ΔnuoΔphaZ* **(C)** with the lens x63. The samples were stained with Nile Red. The samples were harvest 24 h after inoculation and normalized to an OD_{600} of 2.5.

3.4. Relative quantification of PHAs

After confirming the presence of PHA granules inside the mutant strains through fluorescence microscopy, relative quantification of the PHA content of the different working strains was conducted in comparison to the wildtype without the *phaZ* gene, allowing the verification of the influence of the NDHs on the production of PHAs in *P. taiwanensis* VLB120. Two different methods were used to quantify the PHAs. The first method was a rapid quantification method using Nile Red fluorescence and the second approach was based on gas chromatography – mass spectrometry (GC-MS).

3.4.1 Rapid Nile Red method

Before conducting the rapid method with all the working strains, preliminary tests using only three *P. taiwanensis* VLB120 mutant strains were done. These initial experiments allowed the adjustment of the method described in the work of Zuriani and colleagues (Zuriani *et al.* 2013).

3.4.1.1 Preliminary tests

The strains *P. taiwanensis* VLB120*ΔPHA*, *P. taiwanensis* VLB120*ΔΔndhΔphaZ* and *P. taiwanensis* VLB120*ΔnuoΔphaZ* were cultivated overnight in Delft medium and M63 medium. Afterwards, samples were collected and treated as described in Zuriani *et al*., 2013. The cells were placed in 96 wells plates and had their fluorescence intensity measured in a microplate reader, using as emission wavelength 535 nm and as excitation wavelength 615 nm. For each medium, the

fluorescence signal from the control strain, *P. taiwanensis* VLB120*ΔPHA*, were subtracted from the signals of the two working strains.

Figure 19A shows the fluorescence intensity of the two working strains used in the preliminary experiments with different media. As expected, when comparing the fluorescence intensity of each strain in different medium, the cells that grew in M63 medium exhibited more Nile Red fluorescence than the cells that were cultivated in Delft medium. The strain *P. taiwanensis* VLB120*ΔΔndhΔphaZ* had lower fluorescence intensity than the strain *P. taiwanensis* VLB120*ΔnuoΔphaZ*, independently of the culture media. The results also indicated that all of the strains besides the *P. taiwanensis* VLB120*ΔΔndhΔphaZ*, cultivated in Delft medium, had higher fluorescence intensity than the control strain *P. taiwanensis* VLB120*ΔPHA*.

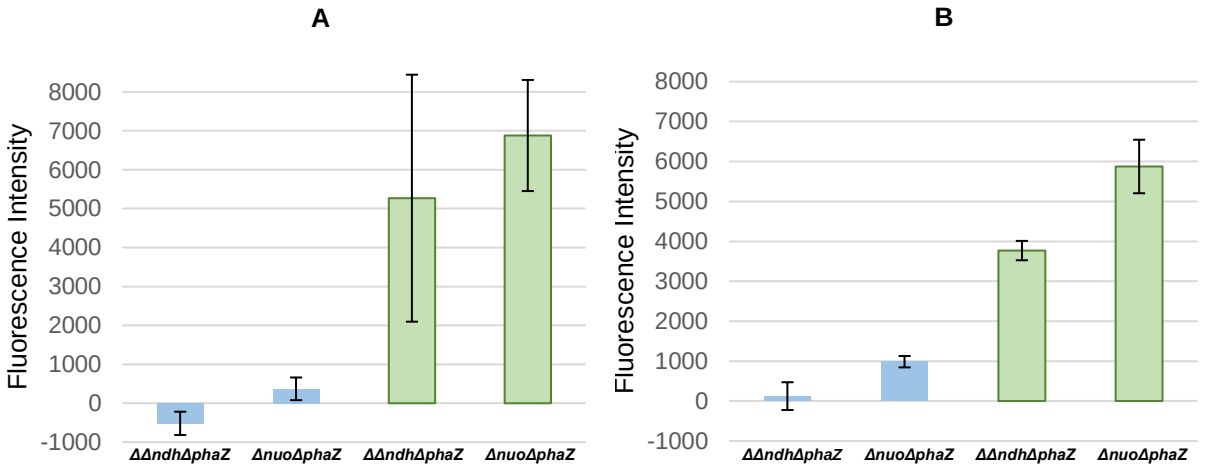

Figure 19. Rapid Nile Red method for quantification of PHAs. The strains *P. taiwanensis* VLB120*ΔnuoΔphaZ* and *P. taiwanensis* VLB120*ΔΔndhΔphaZ* were cultivated overnight in Delft medium (●) and in M63 medium (●). (**A**) corresponds to the results using the Nile Red rapid method with the centrifugation step and (**B**) are the results using the rapid method without the centrifugation step.

In figure 19A the results had a high variance between the triplicates, especially the strains cultivated in M63 medium. To decrease the variance, the procedure was repeated in the same conditions but without the centrifugation step. The modified procedure originated results with the same trends as the original method, but with less variance between the replicas of the strains that grew in M63 medium (figure 19B).

After conducting the preliminary tests, it was decided to apply the Nile Red rapid method, but without the centrifugation step, to all the working strains.

3.4.1.2. Nile Red rapid method with all working strains

The modified Nile Red rapid method was applied to all the NADH-dehydrogenase mutant strains. The working strains were cultivated overnight in Delft medium and, afterwards, submitted to the protocol described in Zuriani *et al.*, 2013, but without the centrifugation step. The figure 20 shows the fluorescence intensity of the different working strains with the signal from the control strain already

subtracted. The fluorescence intensity of the strains *P. taiwanensis* VLB120*ΔphaZ*, *P. taiwanensis* VLB120*Δ13270ΔphaZ*, *P. taiwanensis* VLB120*Δ21880ΔphaZ*, *P. taiwanensis* VLB120*ΔΔndhΔphaZ*, *P. taiwanensis* VLB120*ΔnuoΔphaZ* and *P. taiwanensis* VLB120*ΔnuoΔ13270ΔphaZ* was respectively 443, 146, 573, 78, 1466 and 898.

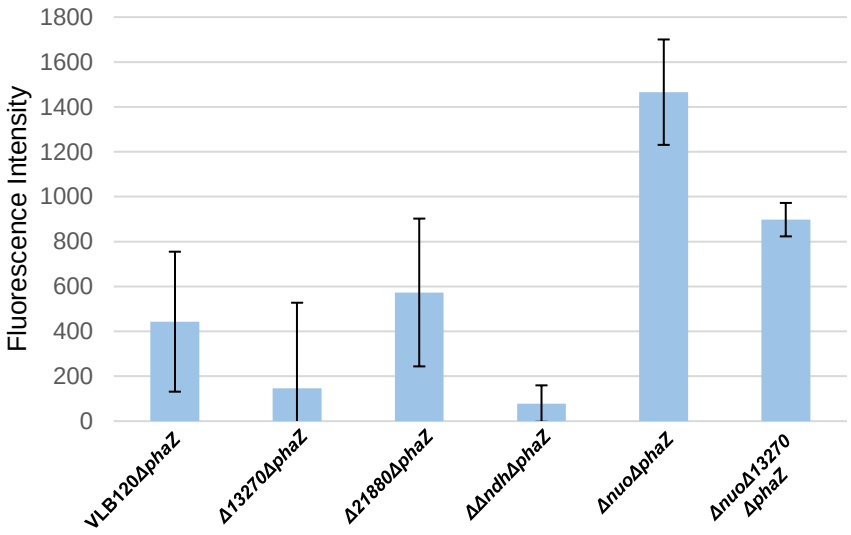

Figure 20. Modified Nile Red rapid method for the relative quantification of PHAs. The strains used for the test were VLB120*ΔphaZ*, *Δ13270ΔphaZ*, *Δ21880ΔphaZ*, *ΔΔndhΔphaZ*, *ΔnuoΔphaZ* and *Δnuo13270ΔphaZ* in Delft medium. The strains *ΔPHA* and VLB120*ΔphaZ* were used as a control and reference, respectively. The fluorescence signal from of the control was subtracted from the signal of the other strains. All the samples were taken in the late stationary phase, 16h after incubation, and normalized to an OD of 0.3.

Next, a relative quantification of the PHA content in percentage was done by comparing the fluorescence intensity of the NADH-dehydrogenase mutants with the strain *P. taiwanensis* VLB120*ΔphaZ* (figure 21). The strains that had a higher PHA content than *P. taiwanensis* VLB120*ΔphaZ*, in descending order, were *P. taiwanensis* VLB120*ΔnuoΔphaZ*, *P. taiwanensis* VLB120*ΔnuoΔ13270ΔphaZ* and *P. taiwanensis* VLB120*Δ21880ΔphaZ* with a percentage of 231%, 103% and 29%, respectively. The strains that had a lower PHA content than P. *taiwanensis* VLB120*ΔphaZ* were *P. taiwanensis* VLB120*Δ13270ΔphaZ* and *P. taiwanensis* VLB120*ΔΔndhΔphaZ* with -82% and -67%, respectively.

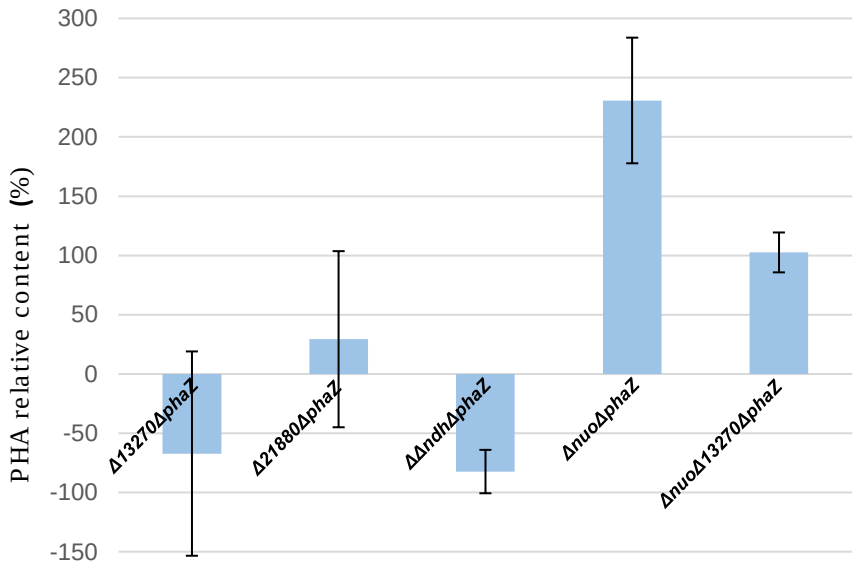

Figure 21. Relative quantification of the PHA content of the NADH-dehydrogenases mutant strains using the modified Nile Red rapid method.

3.4.2. Gas Chromatography – Mass spectrometry (GC-MS)

Besides the Nile Red rapid method, GC-MS was applied to do a relative quantification of the PHA content inside the cells.

All working strains were inoculated in Delft medium, with an initial OD_{600} of 0.1 and harvested after 10-12h of growth corresponding to the stationary phase. The samples were treated as described in the subsection 2.27. and injected in the column of the GC-MS. After analyzing the chromatograms of the different strains, two peaks common to all working strains, besides the control, were identified as being 3-hydroxyoctanoacte (C_8) and 3-hydroxydecanoate (C_{10}). Also, the internal standard used (IS), benzoic acid is clearly visible in the chromatograms. The retention times of benzoic acid, hydroxyoctanoate and 3-hydroxydecanoate were 11.31, 14.89 and 18.99 min, respectively. The areas of the peaks of 3-hydroxyoctanoacte and of 3-hydroxydecanoate (A_{PHA}) were normalized by dividing the areas of the PHAs by the area of the IS (A_{IS}). In figure 22 it can be observed the normalized signals of the different working strains.

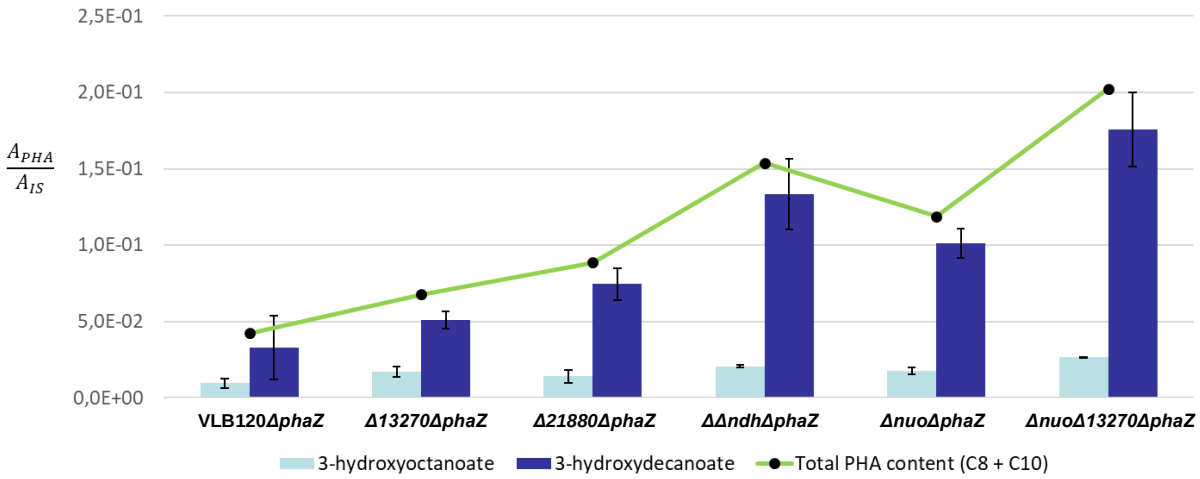

Figure 22. Normalized area of the chromatograms peaks relative to 3-hydroxyoctanoate (C_8) and 3-hydroxydecanoate (C_{10}). The strains used in the experiment were *P. taiwanensis* VLB120*ΔphaZ*, *P. taiwanensis* VLB120*Δ13270ΔphaZ*, *P. taiwanensis* VLB120*Δ21880ΔphaZ*, *P. taiwanensis* VLB120*ΔΔndhΔphaZ*, *P. taiwanensis* VLB120*ΔnuoΔphaZ* and *P. taiwanensis* VLB120*ΔnuoΔ13270ΔphaZ*. The total PHA content was considered as the sum of the normalized area of C_8 and C_{10}. The bacteria grew in minimal medium with 28 mM of glucose.

The GC-MS results show that all the NADH-dehydrogenases mutant strains have a higher PHA content than the strain *P. taiwanensis* VLB120*ΔphaZ*. The strains with the highest PHA content, in descending other, were *P. taiwanensis* VLB120*ΔnuoΔ13270ΔphaZ*, *P. taiwanensis* VLB120*ΔΔndhΔphaZ*, *P. taiwanensis* VLB120*ΔnuoΔphaZ*, *P. taiwanensis* VLB120*Δ21880ΔphaZ* and *P. taiwanensis* VLB120*Δ13270ΔphaZ*. Afterwards, a relative quantification of the PHA content was done between the strain *P. taiwanensis* VLB120*ΔphaZ* and the other NADH-dehydrogenase mutants (figure 23). The strains *P. taiwanensis* VLB120*Δ13270ΔphaZ*, *P. taiwanensis* VLB120*Δ21880ΔphaZ*, *P. taiwanensis* VLB120*ΔΔndhΔphaZ*, *P. taiwanensis* VLB120*ΔnuoΔphaZ* and *P. taiwanensis* VLB120*ΔnuoΔ13270ΔphaZ* produce, respectively, 60%, 109%, 264%, 181% and 379% more than the strain *P. taiwanensis* VLB120*ΔphaZ*. The strains that only had one NADH-dehydrogenase active, *P. taiwanensis* VLB120*ΔnuoΔ13270ΔphaZ* and *P. taiwanensis* VLB120*ΔΔndhΔphaZ* were the cells that had a higher PHA content.

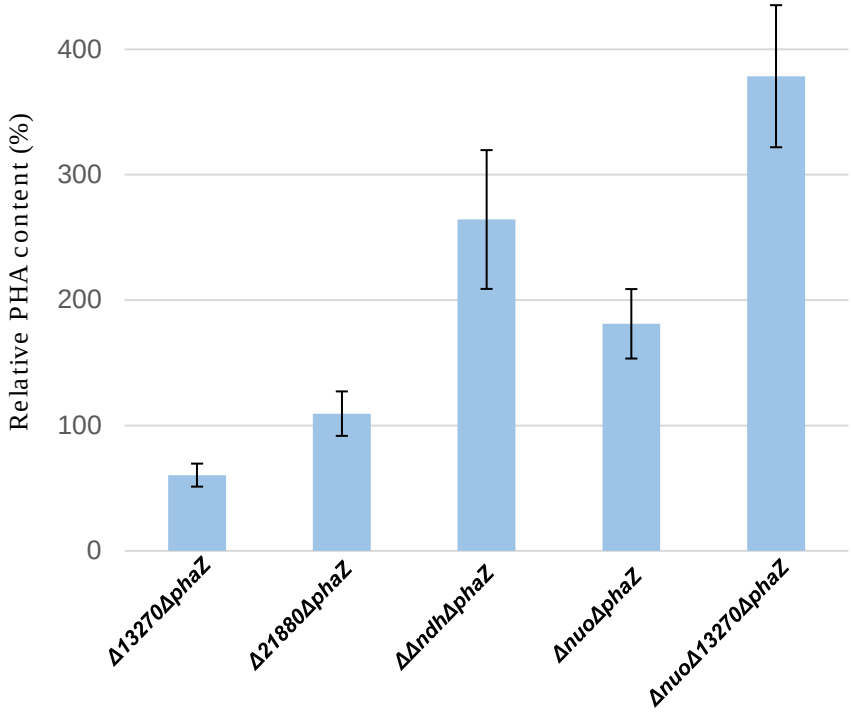

Figure 23. Relative quantification of the PHA content between the strain *P. taiwanensis* VLB120*ΔphaZ* and the NADH-dehydrogenases mutant strains.

4. Discussion

The growth characterization of the NADH-dehydrogenases mutants in Delft medium revealed that only the strain *P. taiwanensis* VLB120*ΔΔndh* had its growth affected, as it can be seen in figure 9. In the stationary phase this strain reached a lower OD_{600} than the wildtype. The cause of this behavior is unknown, since documentation suggests that *Pseudomonas* have a "driven by demand" metabolism. This metabolic behavior consists on the self-regulation of the central carbon metabolism, once there is a need, for example, of more carbon, energy or redox cofactors, to sustain the cells demand, thus avoiding harmful effects on the cell physiology (Ebert *et al.*, 2011). An example of such behavior is, for instance, the strain *P. putida* DOT-T1E that when growing in the presence of a toxic solvent, such as octanol, the strain can match the metabolic demand created by the environment by tripling the glucose uptake rate without producing any secondary products, thus only contributing to the formation of biomass and CO_2 (Blank *et al.,* 2008). All the mutant strains grew with the same amount of glucose, but for some unknown reason the growth of the strain *P. taiwanensis* VLB120*ΔΔndh* was affected. At this point of the project, the experiments suggested that the strain *P. taiwanensis* VLB120*ΔΔndh*, that only has the complex I dehydrogenase activated, was redirecting the metabolic flux from the formation of biomass to the synthesis of PHAs. However, in the following experiments regarding the relative quantification of PHAs between the NDHs mutant strains and the wildtype showed that the strain *P. taiwanensis* VLB120*ΔΔndhΔphaZ* strain does not produce the biggest amount of PHA. The strain *P. taiwanensis* VLB120*ΔnuoΔ13270ΔphaZ* had the highest PHA content of all the strains and a similar growth behavior than the wildtype.

Some of the growth curves of the working strains, like for example the growth curve of *P. taiwanensis* VLB120, seem to have a diauxie in their growth path. This happens because *Pseudomonas* species immediately start oxidizing glucose that is present in the medium into gluconate (Daddaoua *et al.,* 2009). The second diauxic observed is due to the consumption of gluconate by the cells.

Next, the knockout of the PHA depolymerase gene was conducted to all of the working strains (table 8) using the pEMG plasmid system. The gene deletion was performed because on one hand, if the cells undergo carbon starvation they can start consuming PHAs like it is described in the work of Ren and his colleagues (Ren *et al.*, 2009), where the strain *Pseudomonas putida* Gpo1 starts consuming PHAs after reaching the stationary phase. On the other hand, the cells are growing in a minimal medium - Delft – which indicates they are not under any environmental stress that, according to several authors such as Eugenio and her collaborators (Eugenio *et al.,* 2010), would stimulate the production of PHAs, meaning that if the cells produced PHAs due to the NDHs mutations they could consume the polymer right after the beginning of its synthesis.

Fluorescence microscopy experiments with Nile Red were performed using the strains *P. taiwanensis* VLB120*ΔPHA*, *P. taiwanensis* VLB120*ΔphaZ* and *P. taiwanensis* VLB120*ΔnuoΔphaZ*. It can be seen in Figure 18 II that all strains have cells with Nile Red fluorescence, the explanation

behind this has to do with the fact that when the stain permeates the cytoplasmic membrane, it reacts with the lipids inside the cell (Greenspan *et al.,* 1985). However, only the *P. taiwanensis* VLB120*ΔphaZ* and *P. taiwanensis* VLB120*ΔnuoΔphaZ* have present PHA granules. The strain *P. taiwanensis* VLB120*ΔphaZ* (Figure 18 IIB) has significantly less granules than the strain *P. taiwanensis* VLB120*ΔnuoΔphaZ* (Figure 18 IIC), suggesting that the deletion of NADH-dehydrogenases increased the production of PHAs. Figure 18 IIA, shows that strain *P. taiwanensis* VLB120*ΔPHA* only has stained cells without PHA granules, which is a result of the deletion of PHA operon. The fluorescence microscope experiments indicated that the working strains produce PHA granules in Delft medium and they also suggest that the NADH-dehydrogenases affect the production of PHAs. However, the fluorescence microscope experiments do not allow a relative or absolute quantification of the PHA content of the cells. Following experiments were conducted with the intention of allowing a relative quantification between the NADH-dehydrogenases mutants and the *P. taiwanensis* VLB120*ΔphaZ* strain.

The relative quantification of the PHA content of the different strains was achieved using two different methods. The first procedure was a rapid relative quantification method using Nile Red based on the work of Zuriani and collaborators (Zuriani *et al.,* 2013). Preliminary tests were conducted with two strains, *P. taiwanensis* VLB120*ΔΔndhΔphaZ* and *P. taiwanensis* VLB120*ΔnuoΔphaZ*, in two different mediums. At this point in the investigation, the PHA content in the different strains using Delft medium was still unknown, meaning that the PHA content inside the cells could have been not enough to produce a significant signal. To test this hypothesis, a nitrogen limited medium (M63 medium) that induces the production of PHAs, was also used.

The preliminary results using the procedure described by Zuriani and colleagues (Zuriani *et al.,* 2013), are shown in figure 19 A. As predicted, the fluorescence intensity of the strains growing in M63 medium was higher than the signal from the strains that grew in Delft medium. This happens because M63 medium is a nitrogen-limited medium, inducing the production of PHAs. However, still some results were not as expected, like for instance the fluorescence intensity of the strains growing in M63 medium having a significant amount of deviation between the replicas and the signal of the strain *P. taiwanensis* VLB120*ΔΔndhΔphaZ* cultivated in Delft medium being lower than the control strain - *P. taiwanensis* VLB120*ΔPHA*. Nevertheless, by analyzing the experimental procedure, it could be easily figured that the steps of centrifugation and resuspension of the cells were supposed to cause those unexpected results. In this procedure, the cells are normalized to an OD_{600} of 0.3 and during these two steps it is suspected that some biomass is lost. In literature, a similar procedure that also uses Nile Red staining and microplates readers to detect PHAs was found. The work of Cheng and his collaborator (Cheng *et al.,* 2016) describes a similar procedure but without the presence of centrifuge and resuspension steps. After finding this procedure, the preliminary experiments were repeated following the procedure of Zuriani and his colleagues (Zuriani *et al.,* 2013) but without the centrifuge and resuspension steps (figure 19 B). This resulted in a significant improvement of the deviation between the samples grown in M63 medium and in the presence of a higher fluorescence signal of the strain *P. taiwanensis* VLB120*ΔΔndhΔphaZ* when compared to the control strain. After the

preliminaries tests, it was decided to apply the modified method to all the strains in Delft medium, since the control, *P. taiwanensis* VLB120*ΔPHA*, was treated the same way than the rest of the samples, the removal of the centrifugation and resuspension steps should not affect the results.

In figure 20, it can be seen the results associated to the application of the modified Rapid Nile Red method to all the working strains growing in Delft medium. This Nile Red method is a fast procedure however not the most precise. In addition, the lipid content between the strains is unknown and it can significantly affect the results. Thus, following experiments using GC-MS were conducted since they are the most precise that are able to conduct a relative quantification between strains.

The GC-MS chromatograms of the samples from the cell cultures showed the presence of two types of PHA monomers, 3-hydroxyoctanoate and 3-hydroxydecanote. The identification of the different PHAs was done using an online library that compared the ions masses present on the peaks to the mass spectra of known compounds, and searching for the characteristic ions masses of the PHA monomers in each peak. The ions masses characteristic to all MSTFA derivatized PHA monomers are m/z=73 and m/z =89, both originated from the trimethylsilyl group, and m/z=175 that corresponds to the PHA monomer without the side chain (Rijk *et al.*, 2002). The identification of the PHA monomer was done by searching for the signal corresponding to the ion $[M\text{-}15]^+$. In the case of 3-hydroxyoctanoate and 3-hydroxydecanote the ions masses of this signal were m/z=231 and m/z =259, respectively (Klinke *et al.*, 1999). In all chromatograms, the peak area corresponding to poly(3-hydroxydecanoate) was bigger than the area of the peak corresponding to poly(3-hydroxyoctanoate). This corroborates with the theory described in the literature relative to the production of PHAs mainly of the class poly(3-hydroxydecanoate) by *Pseudomonas* when growing in glucose. This can be seen in the work of Huijberts and collaborators (Huijberts *et al.,* 1992), where the strain *Pseudomonas putida* KT2442 accumulated PHAs, which 68.1% were 3-hydroxydecanoate when growing in 2% glucose. A relative PHA quantification between the NADH-dehydrogenases mutant strains and the wildtype was made by considering the total amount of PHA as the sum of the two types of PHA monomers detected in the chromatograms (figure 23). All the NADH-dehydrogenase mutants produce more than the wildtype meaning that the NADH-dehydrogenases affected the PHA production.

The strains that produced more PHA were *P. taiwanensis* VLB120*ΔΔndhΔphaZ* and *P. taiwanensis* VLB120*ΔnuoΔ13270ΔphaZ*. Both strains only have one NADH-dehydrogenase active, *P. taiwanensis* VLB120*ΔΔndhΔphaZ* has the complex I dehydrogenase and *P. taiwanensis* VLB120*ΔnuoΔ13270ΔphaZ* only has the NDH-II coded by the gene *PVLB_21880*. Due to only having one NADH-dehydrogenase activated, these strains are believed to accumulate more NADH than the other strains that have two NADH-dehydrogenases. As explained in the section 1.3 of the introduction, it is believed that the increase in the concentration of NADH inside the cells results in the accumulation of PHAs inside the cells. The strain *P. taiwanensis* VLB120*ΔnuoΔ13270ΔphaZ* produced more PHA than the strain *P. taiwanensis* VLB120*ΔΔndhΔphaZ*. A possible explanation for this difference in the PHA content between the two strains is that the NADH-dehydrogenases have different affinities to the compound NADH. The affinity of the enzyme to its substrate can be evaluated

with respect to the value of the Michaelis constant (K_m). A high value of K_m means that a lot of substrate is needed to saturate the enzyme, indicating a low affinity with the substrate. On the other hand, a low K_m means that only a small amount of substrate is needed in order to saturate the enzyme, meaning that it has a high affinity for the substrate (Cornish-Bowden, 2015) Still, the NADH-dehydrogenases of *P. taiwanensis* VLB120 were not characterized, but the NADH-dehydrogenases between bacteria are homologous and some information regarding these enzymes in other microorganisms is described in the literature. For example, in the strain *E. coli* K-12 MG1655 the K_m for the complex I is 5 μM (Spehr *et al.*, 1999) and for the NDH-II enzyme is 34 μM (Bjorklof *et al,* 2000), which collaborates with the assumption that in *P. taiwanensis* VLB120 the complex I has a higher affinity to NADH than the NDH-II enzyme. All the other strains study have two NADH-dehydrogenases in their genome, being this one the most likely reason why these strains accumulated less PHAs than the other two strains discussed. *P. taiwanensis* VLB120*ΔnuoΔphaZ* is the third most PHA producing strain having both NDH-II enzymes activated. The explanation given before, related to the complex I having possibly a higher affinity to NADH than the NDH-II enzymes also justifies this result. Compared to *P. taiwanensis* VLB120*Δ13270ΔphaZ* and *P. taiwanensis* VLB120*Δ21880ΔphaZ*, *P. taiwanensis* VLB120*ΔnuoΔphaZ* does not possess the complex I, which means it will accumulate more PHA. The strains *P. taiwanensis* VLB120*Δ13270ΔphaZ* and *P. taiwanensis* VLB120*Δ21880ΔphaZ* have both the complex I, but differ on the NDH-II enzyme. The strain *P. taiwanensis* VLB120*Δ13270ΔphaZ* had a lower PHA content than *P. taiwanensis* VLB120*Δ13270ΔphaZ*, suggesting that the NDH-II enzyme coded by the gene *PVLB_21880* has a higher affinity to the substrate than the NDH-II enzyme coded by the gene *PVLB_13270*.

Another possible explanation for the results has to do with the fact that the different NADH-dehydrogenases are not continuously active. Depending on the growth phase of the cells, lag, exponential or stationary phase, different combinations of NADH-dehydrogenases are active.

The rapid Nile Red method suggested different results than the GC-MS. However, the first procedure, which uses Nile Red is a rapid method that it is not as precise as the GC-MS. Furthermore, the differences between the results obtained from the two methods suggest that the lipid content inside the cells is not the same between the different strains. For example, the Nile Red rapid method suggested that strain *P. taiwanensis* VLB120*ΔΔndhΔphaZ* produce almost no PHAs, but in the GC-MS method this strain was the second most producing strain.

5. Conclusions and future remarks

The development of the present investigation allowed the study of the influence of NADH-dehydrogenases on PHA production in *P. taiwanensis* VLB120. Several mutants were used with different combinations of NADH-dehydrogenases. The strain *P. taiwanensis* VLB120*ΔΔndh* exhibited a growth behavior different than the other working strains by reaching a lower OD_{600} in the stationary phase. The reasons behind these results are not know, however these results were crucial to show that the deletion of NADH-dehydrogenases can affect the behavior of the cells.

The deletion of the PHA depolymerase gene guaranteed that the cells would not consume the PHAs. In all the experiments the cells grew in Delft medium without an environmental stress. This could constitute a problem when making a relative quantification of the PHA content of the different working strains, since there was no conclusion regarding the possible degradation of PHAs by the cells when growing in a minimal medium.

Fluorescence microscopy using Nile Red showed to be effective for the observation of the PHA content inside the cells. The mutant *P. taiwanensis* VLB120*ΔnuoΔphaZ* had numerous cells with fluorescence granules and considerably more than the strain *P. taiwanensis* VLB120*ΔphaZ*. These results justified the advances made in the present research that lead to the application of analytical methods that allowed a relative quantification of the PHA content of the NADH-dehydrogenases mutants and the wildtype. Two different methods were used to make a relative quantification of the PHA content inside the cells; one was based on the Nile Red fluorescence and the other one on GC-MS.

By using GC-MS, two different types of PHA monomers were detected in the cells, 3-hydroxyoctanoates and 3-hydroxydecanoates (supplemental data, S.IV.). However, most of the monomers were 3-hydroxydecanoate (figure 22) which goes accordingly with what is described in the literature related to the production of PHAs using *Pseudomonas* strains and glucose as carbon source. All the NADH-dehydrogenases mutant strains produced more PHAs than the wildtype, which shows that the NADH-dehydrogenases influenced the production of PHAs in the strain *P. taiwanensis* VLB120. The strains *P. taiwanensis* VLB120*ΔnuoΔ13270ΔphaZ* and *P. taiwanensis* VLB120*ΔΔndhΔphaZ* had the highest PHA content, producing, respectively, 379% and 264% more than the wildtype. The other strains *P. taiwanensis* VLB120*Δ13270ΔphaZ*, *P. taiwanensis* VLB120*Δ21880ΔphaZ* and *P. taiwanensis* VLB120*ΔnuoΔphaZ* produced, respectively, 60%, 109% and 181% more when compared to the wildtype. These results indicate the possibility of the NADH-dehydrogenases possessing different affinities to NADH. In ascending order of affinity to the substrate: NDH-II *PVLB_13270*, NDH-II *PVLB_21880* and complex I.

The rapid Nile Red method showed to be an unreliable procedure to compare the PHA content among the working strains. GC-MS is the most precise method available to measure the PHA content inside the cells and the results obtained with this analytical procedure and the rapid Nile Red method

do not show the same tendency. These differences suggest that the lipid content in the different working strains varies enough to enable contradictory results between the two methods.

In the end, the ultimate goal of this work was achieved. The influence of NADH-dehydrogenases on PHA production in *P. taiwanensis* VLB120 was studied successfully. However, there is still more experiments and research that can be conducted with the intention of obtaining more detailed information about the NADH-dehydrogenases and their influence in PHA production. First, the relative quantification using GC-MS was done without the use of standards. The identification of PHA monomers was done by manually analyzing the peaks of the chromatograms, looking for the characteristic ions masses of the PHAs monomers, and comparing the ions masses of the peaks to an online library of known compounds. The use of standards would confirm the identification of the PHA monomers and enable the possibility of doing an absolute quantification. Furthermore, the samples used for the relative quantification of PHAs were collected once the cells had just entered the stationary phase, but in order to confirm the hypothesis that the three NADH-dehydrogenases, of *P. taiwanensis* VLB120, are not always active at the same time, it is required to collect samples at different growth phases of the cells. For example, it would be interesting to sample at the end of the lag phase and on the middle of the exponential phase, near the depletion of glucose in the medium. Additionally, the determination of the kinetic properties of the NADH-dehydrogenases present in *P. taiwanensis* VLB120 is necessary to confirm the affinity of these enzymes to the substrate NADH. Finally, as an extra to the main goal of the project, it could be studied the influence of the NADH-dehydrogenases in industrial PHA producing strains, such as *Ralstonia eutropha* and *Pseudomonas putida* S12.

6. References

Archer, C. D. and Elliott, T. (1995) 'Transcriptional control of the *nuo* operon which encodes the energy-conserving NADH dehydrogenase of *Salmonella typhimurium*.', Journal of bacteriology, 177(9), pp. 2335–2342.

Berrisford, J. M., Baradaran, R. and Sazanov, L. A. (2016) 'Biochimica et Biophysica Acta Structure of bacterial respiratory complex I', BBA - Bioenergetics. Elsevier B.V., 1857(7), pp. 892–901.

Bjorklof, K., Zickermann, V. and Finel, M. (2000) 'Purification of the 45 kDa, membrane bound NADH dehydrogenase of *Escherichia coli* (NDH-2) and analysis of its interaction with ubiquinone analogues', FEBS Letters, 467(1), pp. 105–110.

Blank, L. M., Ionidis, G., Ebert, B. E., Bühler, B. and Schmid, A. (2008) 'Metabolic response of *Pseudomonas putida* during redox biocatalysis in the presence of a second octanol phase', FEBS Journal, 275(20), pp. 5173–5190.

Cheng, J. and Charles, T. C. (2016) 'Novel polyhydroxyalkanoate copolymers produced in *Pseudomonas putida* by metagenomic polyhydroxyalkanoate synthases', Applied Microbiology and Biotechnology. Applied Microbiology and Biotechnology, 100(17), pp. 7611–7627.

Chomczynski, P. and Rymaszewski, M. (2006) 'Alkaline polyethylene glycol-based method for direct PCR from bacteria, eukaryotic tissue samples, and whole blood', BioTechniques, 40(4), pp. 454–458.

Cornish-Bowden, A. (2015) 'One hundred years of Michaelis–Menten kinetics', Perspectives in Science. Elsevier, 4, pp. 3–9.

Daddaoua, A., Krell, T. and Ramos, J. L. (2009) 'Regulation of glucose metabolism in *Pseudomonas*. The phosphorylative branch and Entner-Doudoroff enzymes are regulated by a repressor containing a sugar isomerase domain', Journal of Biological Chemistry, 284(32), pp. 21360–21368.

Ebert, B. E., Kurth, F., Grund, M., Blank, L. M. and Schmid, A. (2011) 'Response of *Pseudomonas putida* KT2440 to increased NADH and ATP demand', Applied and Environmental Microbiology, 77(18), pp. 6597–6605.

Escapa, I. F., García, J. L., Bühler, B., Blank, L. M. and Prieto, M. A. (2012) 'The polyhydroxyalkanoate metabolism controls carbon and energy spillage in *Pseudomonas putida'*, Environmental Microbiology, 14(4), pp. 1049–1063.

De Eugenio, L. I., Escapa, I. F., Morales, V., Dinjaski, N., Galán, B., García, J. L. and Prieto, M. A. (2010) 'The turnover of medium-chain-length polyhydroxyalkanoates in *Pseudomonas putida* KT2442 and the fundamental role of PhaZ depolymerase for the metabolic balance', Environmental Microbiology, 12(1), pp. 207–221.

Friedrich, T. and Scheide, D. (2000) 'The respiratory complex I of bacteria, archaea and eukarya and its module', Febs Letters, 479(1 / 2), p. 1.

Greenspan, P., Mayer, E. P. and Fowler, S. D. (1985) 'Nile red: a selective fluorescent stain for intracellular lipid droplets, J. Cell Biol. 100 (1985) 965–973.', The Journal of Cell Biology, 100(10), pp. 965–973.

Halan, B., Schmid, A. and Buehler, K. (2011) 'Real-time solvent tolerance analysis of *Pseudomonas sp.* Strain VLB120*ΔC* catalytic biofilms', Applied and Environmental Microbiology, 77(5), pp. 1563–1571.

Heikal, A., Nakatani, Y., Dunn E., Weimar, M. R., Day, C. L., Baker, E. N., Lott, J. S., Sazanov, L. A. and Cook, G. M. (2014) 'Structure of the bacterial type II NADH dehydrogenase: A monotopic membrane protein with an essential role in energy generation', Molecular Microbiology, 91(5), pp. 950–964.

Huijberts, G. N. M., Eggink, G., De Waard, P., Huisman, G. W. and Witholt, B. (1992) '*Pseudomonas putida* KT2442 cultivated on glucose accumulates poly(3-hydroxyalkanoates) consisting of saturated and unsaturated monomers', Applied and Environmental Microbiology, 58(2), pp. 536–544.

Jiang, G., Hill, D. J., Kowalczuk, M., Johnston, B., Adamus, G., Irorere, V. and Radecka, I. 'Carbon sources for polyhydroxyalkanoates and an integrated biorefinery', International Journal of Molecular Sciences, 17(7).

Kerscher, S., Dröse, S., Zickermann, V. and Brandt, U. (2008) 'The three families of respiratory NADH dehydrogenases', Results and Problems in Cell Differentiation, 45(May), pp. 185–222.

Klinke, S., Ren Q., Witholt, B. and Kessler, B. (1999) 'Production of Medium-Chain-Length Poly (3-Hydroxyalkanoates) from Gluconate by Recombinant *Escherichia coli'*, 65(2), pp. 540–548.

Köhler, K. A. K., Rückert, C., Schatschneider, S., Vorhölter, F. J., Szczepanowski, R., Blank, L. M., Niehaus, K., Goesmann, A., Pühler, A., Kalinowski, J. and Schmid, A. (2013) 'Complete genome sequence of *Pseudomonas sp.* strain VLB120 a solvent tolerant, styrene degrading bacterium, isolated from forest soil', Journal of Biotechnology. Elsevier B.V., 168(4), pp. 729–730.

Köhler, K. A. K., Blank, L. M., Frick, O. and Schmid, A. (2015) 'D-Xylose assimilation via the Weimberg pathway by solvent-tolerant *Pseudomonas taiwanensis* VLB120', Environmental Microbiology, 17(1), pp. 156–170.

Lee, S. Y. (1996) 'Bacterial Polyhydroxyalkanoates', Biotechnology and bioengineering, 49, pp. 1–14.

Martínez-García, E. and de Lorenzo, V. (2011) 'Engineering multiple genomic deletions in Gram-negative bacteria: Analysis of the multi-resistant antibiotic profile of *Pseudomonas putida* KT2440', Environmental Microbiology, 13(10), pp. 2702–2716.

Matsushita, K., Yamada, M., Shinagawa, E., Adachi, O. and Ameyama, M. (1980) 'Membrane-bound respiratory chain of *Pseudomonas aeruginosa* grown aerobically', Journal of Bacteriology, 141(1), pp. 389–392.

Reddy, C. S. K., Ghai, R., Rashmi, Kalia, V. C. (2003) 'Polyhydroxyalkanoates: An overview', Bioresource Technology, 87(2), pp. 137–146.

Ren, Q., de Roo, G., Ruth K., Witholt, B., Zinn, M. and Thöny, L. (2009) 'Simultaneous accumulation and degradation of polyhydroxyalkanoates: Futile cycle or clever regulation?', Biomacromolecules, 10(4), pp. 916–922.

Gel'man, N. S., Lukoyanova M. A. and Ostrovskii D. N. (1967) 'Respiration and Phosphorylation of Bacteria', Moscow, Springer Science + Business Media, LLC.

de Rijk, T. C., de Meer, P., Eggink G., Weusthuis, R. A. 'Methods for Analysis of Poly (3-hydroxyalkanoate) (PHA) Composition', Biopolymers, 3b, pp. 1–12.

Sackett, D. L. and Wolff, J. (1987) 'Nile red as a polarity-sensitive fluorescent probe of hydrophobic protein surfaces', Analytical Biochemistry, 167(2), pp. 228–234.

Schmitz, S., Nies, S., Wierckx, N., Blank, L. M. and Rosenbaum, M. A. (2015) 'Engineering mediator-based electroactivity in the obligate aerobic bacterium *Pseudomonas putida* KT2440', Frontiers in Microbiology, 6(APR), pp. 1–13.

Spehr, V., Schlitt, A., Scheide, D., Guénebaut, V. and Friedrich, T. (1999) 'Overexpression of the *Escherichia coli nuo*-Operon and Isolation of the Overproduced NADH: Ubiquinone Oxidoreductase (Complex I)', Biochemistry, 38, pp. 16261–16267.

Tan, G. Y. A., Chen, C., Li, L., Ge, L., Wang, L., Razaad, I. M. N., Li, Y., Zhao, L., Mo, Y. and Wang, J. (2014) 'Start a research on biopolymer polyhydroxyalkanoate (PHA): A review', Polymers, 6(3), pp. 706–754.

Volmer, J., Neumann, C., Bühler, B. and Schmid, A. (2014) 'Engineering of *Pseudomonas taiwanensis* VLB120 for constitutive solvent tolerance and increased specific styrene epoxidation activity', Applied and Environmental Microbiology, 80(20), pp. 6539–6548.

Wu, H., Sheu, D. and Lee, C. (2003) 'Rapid differentiation between short-chain-length and bacteria with spectrofluorometry', 53, pp. 131–135.

Zuriani, R., Vigneswari, S., Azizan, M. N. M., Majid, M. I. A. and Amirul, A. A. (2013) 'A high throughput Nile red fluorescence method for rapid quantification of intracellular bacterial polyhydroxyalkanoates', Biotechnology and Bioprocess Engineering, 18(3), pp. 472–478.

7. Supplemental data

S.I. Growth curves of the working strains

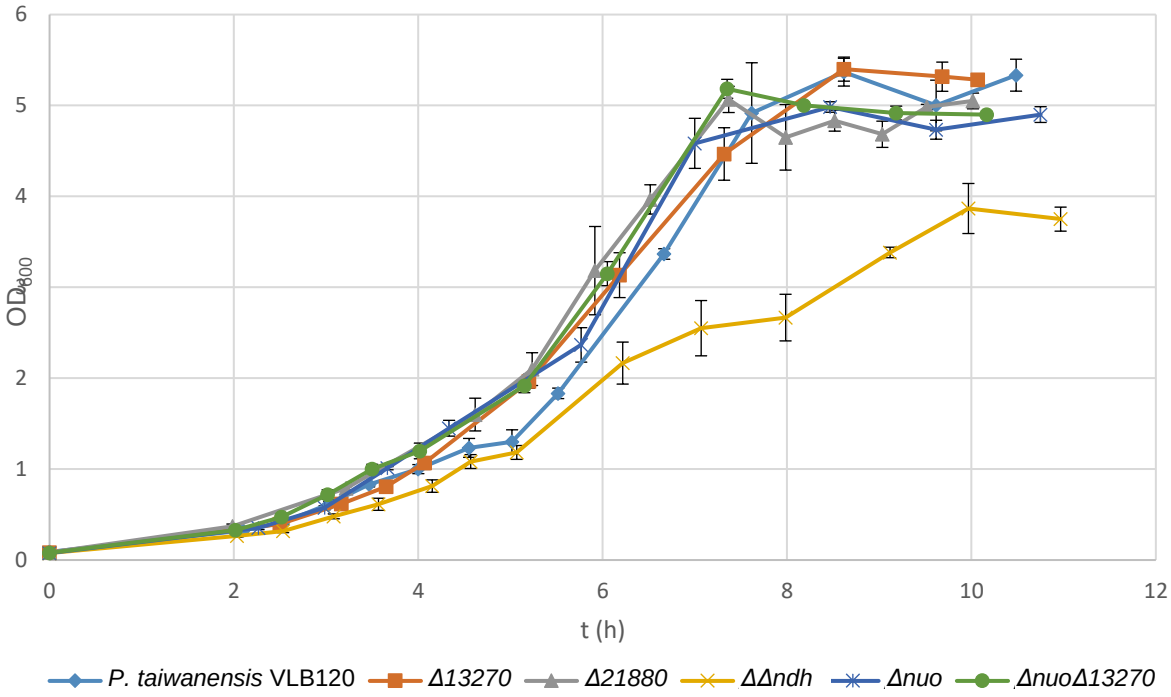

Figure S1. Growth curve experiments of *P. taiwanensis* VLB120, *P. taiwanensis* VLB120*Δ13270*, *P. taiwanensis* VLB120*Δ21880*, *P. taiwanensis* VLB120*ΔΔndh*, *P. taiwanensis* VLB120*Δnuo* and *P. taiwanensis* VLB120*ΔnuoΔ13270*. The *Pseudomonas* strains were cultivated in minimal medium (Delft), with 25 mM of glucose, at 30 ºC at a shaking velocity of 300 rpm.

S.II. Integration of the construct pEMG-TS1/TS2

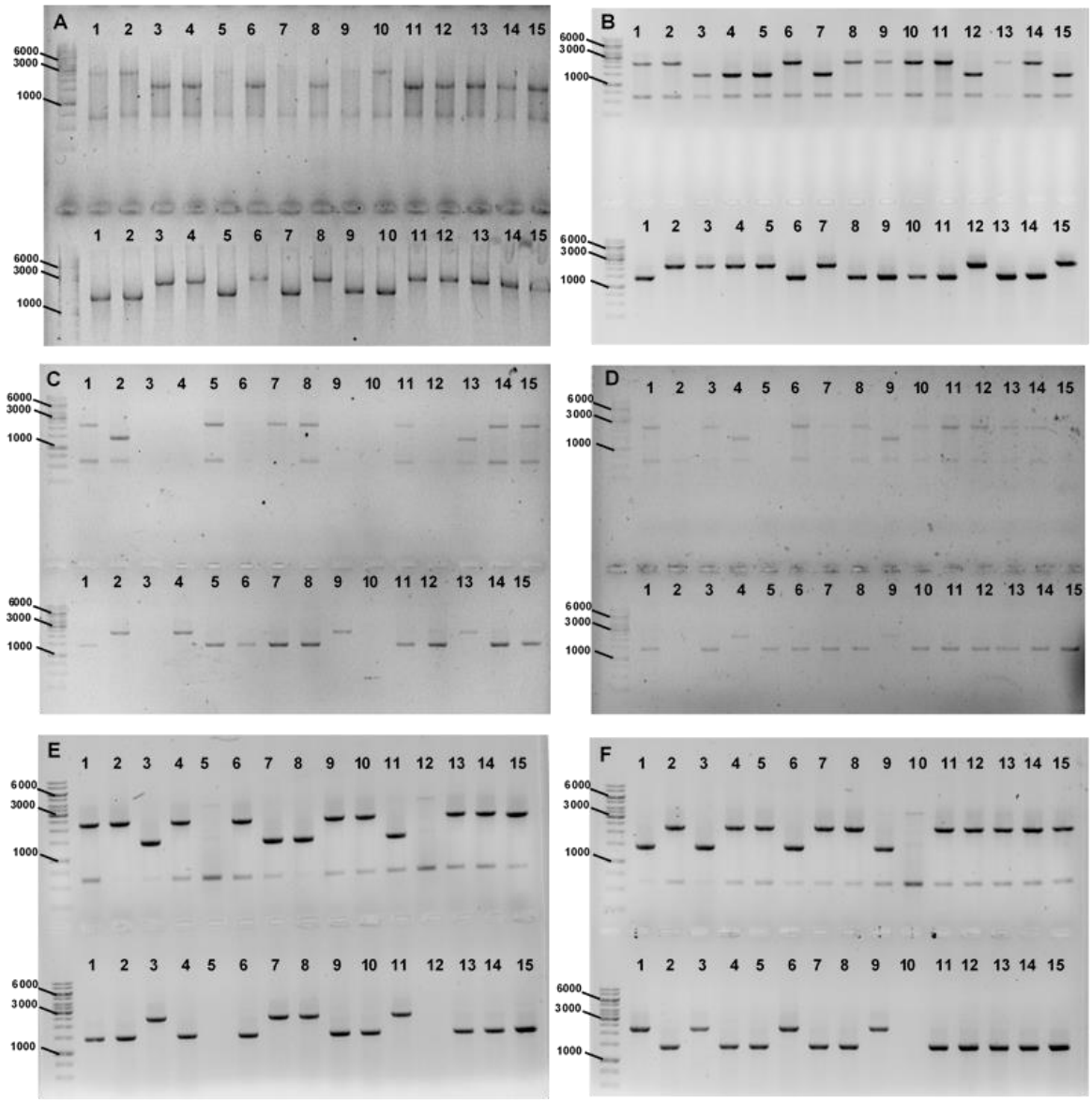

Figure S2. Confirmation of the insertion of the construct pEMG – TS1/TS2 into the genome of the strains P. *taiwanensis* VLB120 (**A**), *P. taiwanensis* VLB120*Δ13270* (**B**), *P. taiwanensis* VLB120*Δ21880* (**C**), *P. taiwanensis* VLB120*ΔΔndh* (**D**), *P. taiwanensis* VLB120*Δnuo* (**E**) and *P. taiwanensis* VLB120*ΔnuoΔ13270* (**F**). The upper part of each gel is a colony PCR where the primers SN192 and BW014 were used and the bottom part of the gels are the colony PCR results using the primers BW013 and SN193. The numbers #1 to #15 represent different colonies of each strain. In the first lane is present the gene ruler 1 kb DNA ladder (Fermentas) with indicated sizes in base pairs.

S.III. Confirmation of the knockout of the PHA depolymerase gene

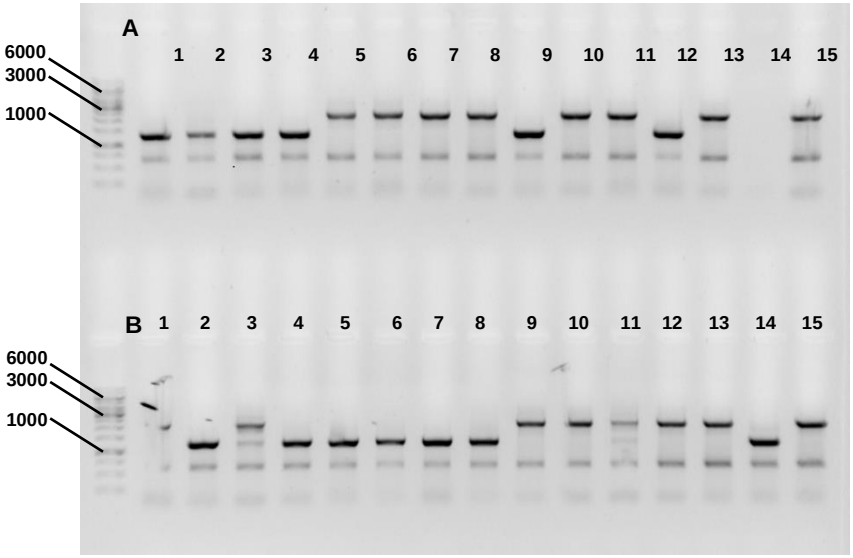

Figure S3. Confirmation of the knockout of the target gene of the strains *P. taiwanensis* VLB120 wildtype (A) and *P. taiwanensis* VLB120*Δ13270* (B). If the knockout of the target gene was a success the PCR result will have a DNA fragment with about 1255 bp. Otherwise, the PCR result will have a fragment size of approximately 2113 bp corresponding to the wildtype. The numbers #1 to #15 represent different colonies of each strain. In the first lane is present the gene ruler 1 kb DNA ladder (Fermentas) with indicated sizes in base pairs.

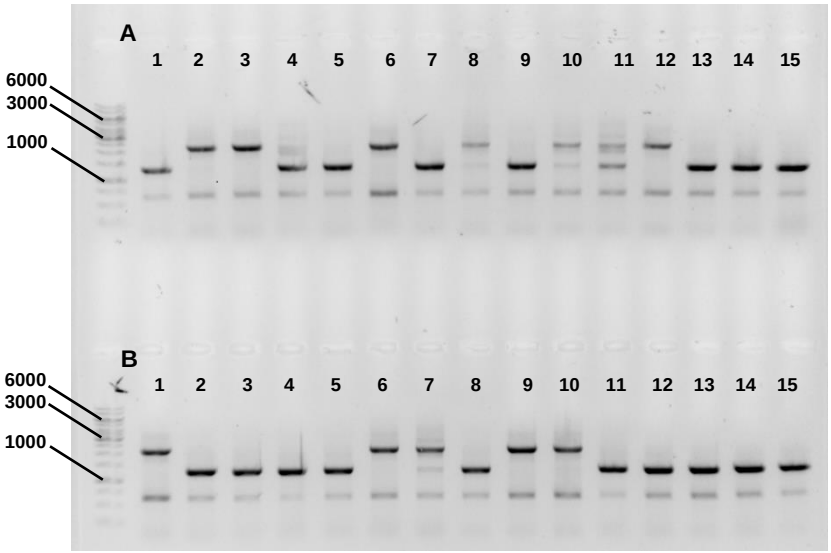

Figure S4. Confirmation of the knockout of the target gene of the strains *P. taiwanensis* VLB120*Δ21880* (A) and *P. taiwanensis* VLB120*ΔΔndh* (B). If the knockout of the target gene was a success the PCR result will have a DNA fragment with approximately 1255 bp. Otherwise, the PCR result will have a fragment size of about 2113 bp corresponding to the wildtype. The numbers #1 to #15 represent different colonies of each strain. In the first lane is present the gene ruler 1 kb DNA ladder (Fermentas) with indicated sizes in base pairs.

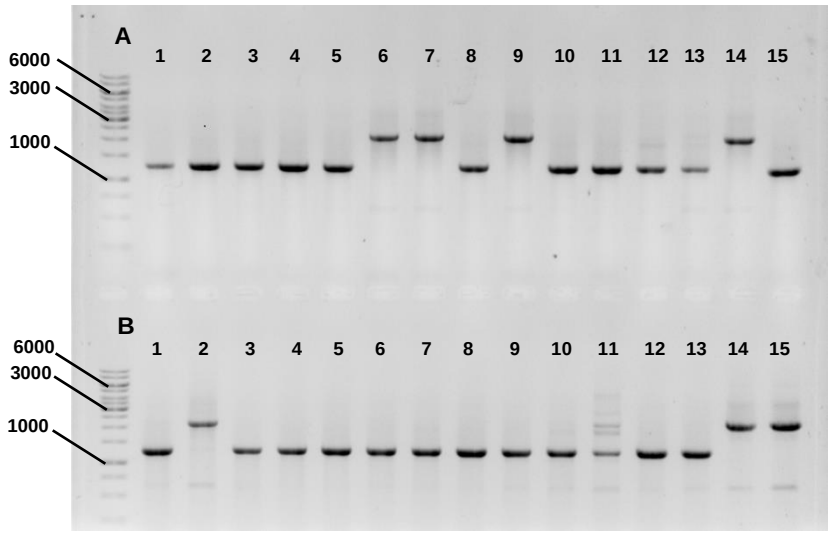

Figure S5. Confirmation of the knockout of the target gene of the strains *P. taiwanensis* VLB120*Δnuo* (A) and *P. taiwanensis* VLB120*ΔnuoΔ13270* (B). If the knockout of the target gene was a success the PCR result will have a DNA fragment with about 1255 bp. Otherwise, the PCR result will have a fragment size of approximately 2113 bp corresponding to the wildtype. The numbers #1 to #15 represent different colonies of each strain. In the first and last lane of the agarose gel is present the gene ruler 1 kb DNA ladder (Fermentas) with indicated sizes in base pairs.

S.IV. Chromatograms of the working strains

Only one chromatogram of each working strain is shown.

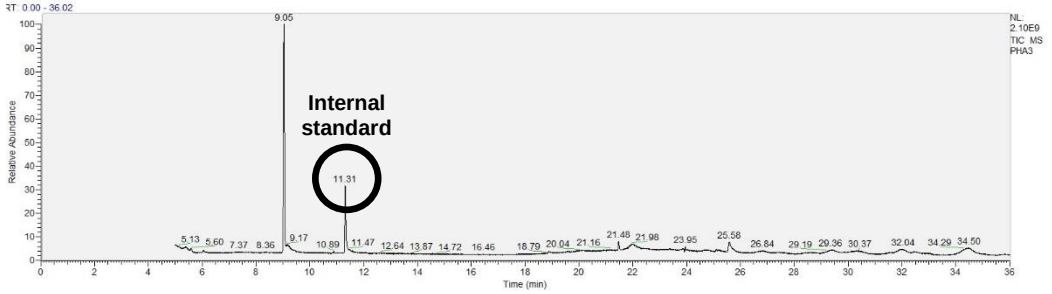

Figure S6. Chromatogram of the control strain *P. taiwanensis* VLB120*ΔPHA*. Only the internal standard, benzoic acid, is present with a retention time of 11.31 minutes.

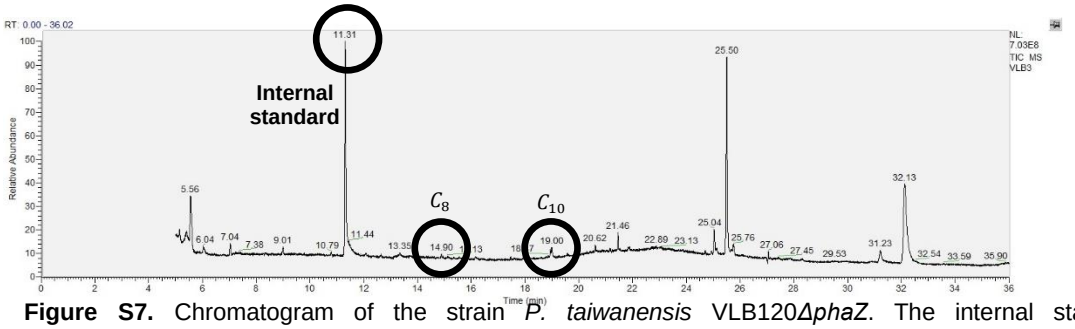

Figure S7. Chromatogram of the strain *P. taiwanensis* VLB120*ΔphaZ*. The internal standard, 3-hydroxyoctanoate (C_8) and 3-hydroxydecanoate (C_{10}) are present with a retention time of 11.31, 14.90 and 19.00 minutes.

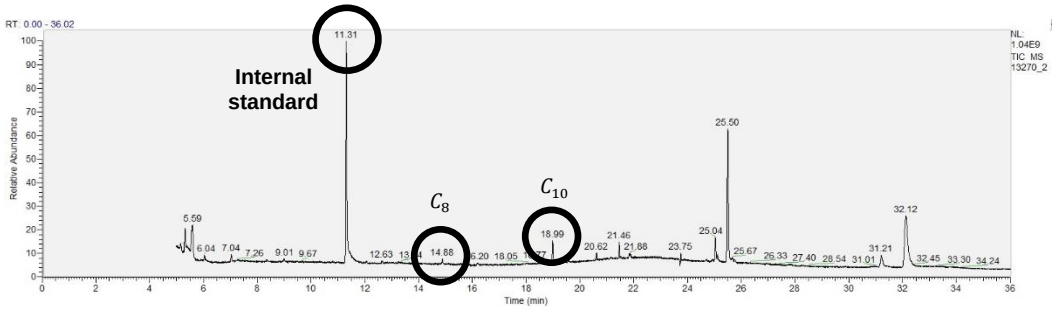

Figure S8. Chromatogram of the strain *P. taiwanensis* VLB120*Δ13270ΔphaZ*. The internal standard, 3-hydroxyoctanoate (C_8) and 3-hydroxydecanoate (C_{10}) are present with a retention time of 11.31, 14.88 and 18.99 minutes.

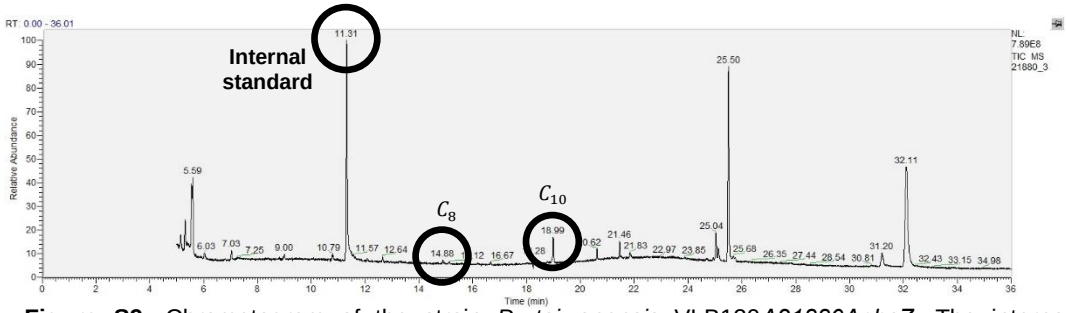

Figure S9. Chromatogram of the strain *P. taiwanensis* VLB120*Δ21880ΔphaZ*. The internal standard, 3-hydroxyoctanoate (C_8) and 3-hydroxydecanoate (C_{10}) are present with a retention time of 11.31, 14.88 and 18.99 minutes.

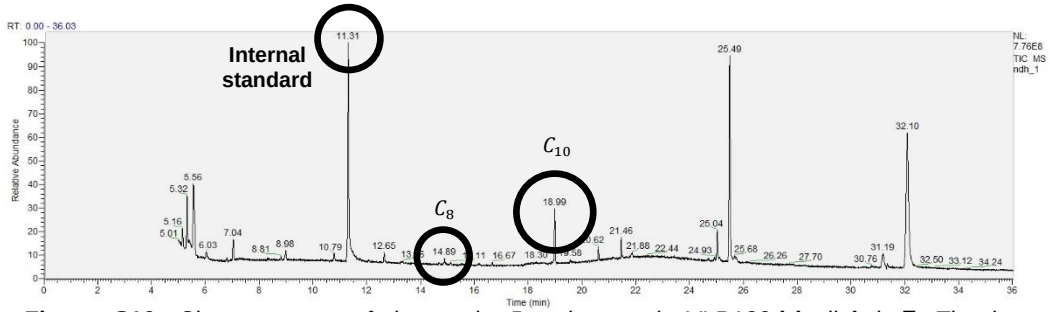

Figure S10. Chromatogram of the strain *P. taiwanensis* VLB120*ΔΔndhΔphaZ*. The internal standard, 3-hydroxyoctanoate (C_8) and 3-hydroxydecanoate (C_{10}) are present with a retention time of 11.31, 14.89 and 18.99 minutes.

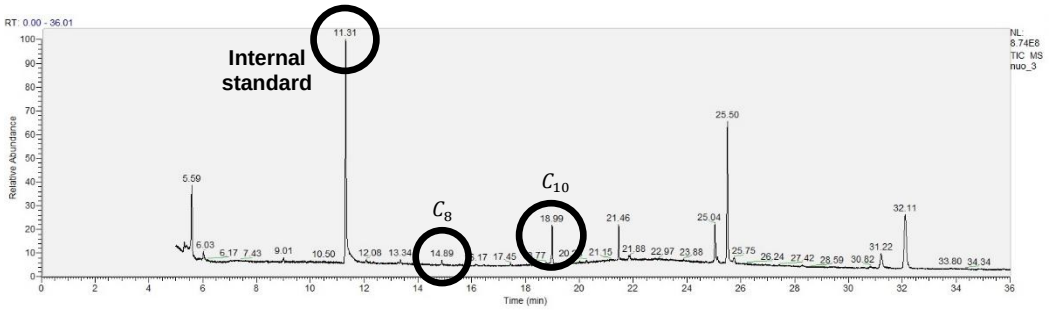

Figure S11. Chromatogram of the strain *P. taiwanensis* VLB120*ΔnuoΔphaZ*. The internal standard, 3-hydroxyoctanoate (C_8) and 3-hydroxydecanoate (C_{10}) are present with a retention time of 11.31, 14.89 and 18.99 minutes.

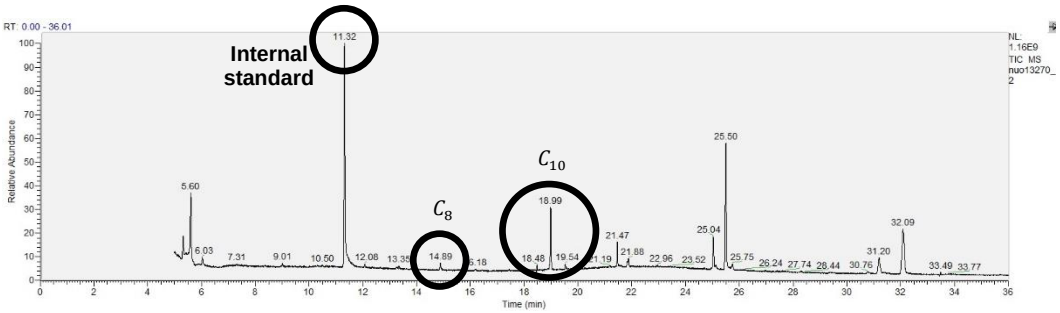

Figure S12. Chromatogram of the strain *P. taiwanensis* VLB120*ΔnuoΔ13270ΔphaZ*. The internal standard, 3-hydroxyoctanoate (C_8) and 3-hydroxydecanoate (C_{10}) are present with a retention time of 11.32, 14.89 and 18.99 minutes.